Early Mars hydrology: Meridiani playa deposits and the sedimentary record of Arabia Terra

Citation: Andrews-Hanna, Jeffrey C. et al. "Early Mars Hydrology: Meridiani Playa Deposits and the Sedimentary Record of Arabia Terra." Journal of Geophysical Research 115.E6 (2010): n. pag. Web. ©2010 American Geophysical Union.

As Published: http://dx.doi.org/10.1029/2009je003485

Publisher: American Geophysical Union

Persistent URL: http://hdl.handle.net/1721.1/74246

Version: Final published version: final published article, as it appeared in a journal, conference proceedings, or other formally published context

JOURNAL OF GEOPHYSICAL RESEARCH, VOL. 115, E06002, doi:10.1029/2009JE003485, 2010

Early Mars hydrology: Meridiani playa deposits and the sedimentary record of Arabia Terra

Jeffrey C. Andrews-Hanna,[1] Maria T. Zuber,[2] Raymond E. Arvidson,[3] and Sandra M. Wiseman[3]

Received 31 July 2009; revised 14 November 2009; accepted 5 January 2010; published 5 June 2010.

[1] The Meridiani Planum region of Mars has been identified as a region of past aqueous activity by a combination of orbital and in situ observations that revealed evidence for sulfate-rich dirty evaporites formed in a playa setting. We investigate the hydrology and sedimentary record of this area using global and regional hydrological models in which groundwater flow is driven by a combination of precipitation, evaporation, and the surface topography. Groundwater evaporation results in evaporite precipitation and cementation of aeolian sediments, allowing the accumulation of deposits of substantial thickness, which then affect the subsequent patterns of groundwater flow. Hydrological activity is initially predicted to be isolated to the deepest craters and depressions, primarily within the Arabia Terra region surrounding Meridiani. As these depressions fill with sediments, the groundwater upwelling spreads laterally across broad regions of Arabia Terra, including Meridiani Planum, as well as regional topographic lows such as the northern lowlands and large impact basins. The model predictions are borne out by observations of large intracrater deposits, inverted valley networks, finely layered deposits, spectral evidence for hydrated sulfates, and pedestal craters that preserve the remnants of a much larger deposit that once covered much of Arabia Terra. The results suggest that the inferred playa at Meridiani was part of a regionally extensive zone of groundwater upwelling. This hydrological cycle requires that conditions in the late Noachian to early Hesperian must have been conducive to the existence of liquid water at the surface throughout much of the low latitudes of Mars.

Citation: Andrews-Hanna, J. C., M. T. Zuber, R. E. Arvidson, and S. M. Wiseman (2010), Early Mars hydrology: Meridiani playa deposits and the sedimentary record of Arabia Terra, *J. Geophys. Res.*, *115*, E06002, doi:10.1029/2009JE003485.

1. Introduction

[2] The surface of early Mars, like that of the Earth today, was shaped by an active hydrological cycle involving liquid water at and below the surface. The nature of the early hydrological cycle is thus far best revealed at Meridiani Planum, where a combination of orbital and in situ observations have revealed abundant evidence for water at an unprecedented level of detail. Early observations by the Mars Global Surveyor (MGS) Thermal Emission Spectrometer (TES) revealed this region of Mars to be mineralogically unique as the primary concentration of hematite, a mineral commonly associated with aqueous processes [*Christensen et al.*, 2000, 2001]. At the same time, high resolution images from the MGS Mars Orbiter Camera (MOC) revealed finely layered rocks of apparent sedimentary origin concentrated in this region of Mars [*Malin and Edgett*, 2000].

[3] Motivated by these observations, the Mars Exploration Rover Opportunity was sent to explore this area, and provided the first clear in situ evidence for the persistent presence of liquid water on the surface of early Mars. The rover observations revealed that the hematite is present as a lag deposit of concretions concentrated above an eroding sedimentary deposit. Outcrops of the deposit exhibit both aeolian and fluvial sedimentary structures [*Grotzinger et al.*, 2005], with the grains themselves composed of a mixture of sulfate salts and weathered basalt. The primary evaporite mineralogy of the grains and the secondary reworked sedimentary structures have been overprinted by tertiary episodes of groundwater-mediated diagenesis that were responsible for the formation of the hematite concretions, the cementation and alteration of the deposits, and the formation and dissolution of mineral clasts to leave behind tabular voids [*Grotzinger et al.*, 2005; *McLennan et al.*, 2005; *Squyres and Knoll*, 2005].

[4] The Meridiani deposits have been interpreted as the remains of an ancient playa in which dirty evaporites formed

[1]Department of Geophysics and Center for Space Resources, Colorado School of Mines, Golden, Colorado, USA.
[2]Department of Earth, Atmospheric, and Planetary Sciences, Massachusetts Institute of Technology, Cambridge, Massachusetts, USA.
[3]Department of Earth and Planetary Sciences, Washington University in St. Louis, St. Louis, Missouri, USA.

0148-0227/10/2009JE003485

in interdune depressions, were subjected to intensive aeolian and fluvial reworking, and were then diagenetically modified by a fluctuating water table [*Grotzinger et al.*, 2005; *McLennan et al.*, 2005; *Squyres and Knoll*, 2005; *Arvidson et al.*, 2006a]. The formation of these deposits and their accumulation to thicknesses approaching 1 km must have been accompanied and driven by a regional rise in the water table [*Arvidson et al.*, 2006a]. These interpretations are bolstered by the association of similar sulfate and hematite deposits with locations of known groundwater outflow in the chaos regions and canyons at the source of the outflow channels [*Glotch and Rogers*, 2007]. Both the specific interpretations of the observed deposits in Meridiani and the mechanisms invoked to produce them have been challenged by several alternative views [*Knauth et al.*, 2005; *McCollom and Hynek*, 2005; *Niles and Michalski*, 2009]. Nevertheless, the full suite of sedimentological and mineralogical evidence is best explained by deposition of the sediments within a playa. In this work, we focus primarily on understanding the processes responsible for the inferred playa deposit, and only briefly address these alternative interpretations.

[5] Meridiani Planum itself is part of a larger high thermal inertia, light toned unit that is likely of similar provenance, referred to as the etched terrain [*Hynek*, 2004]. In addition to the deposits in Meridiani, widespread layered deposits of apparent sedimentary origin are seen throughout Arabia Terra. Originally identified as a mantling unit [*Moore*, 1990], higher resolution MOC images revealed the deposits to consist of finely layered sedimentary rocks [*Malin and Edgett*, 2000; *Edgett and Malin*, 2002]. Evidence for cementation and induration of the deposits suggests that liquid water likely played a role in their deposition or modification [*Fassett and Head*, 2007]. Morphological similarity and direct continuity of these Arabia Terra deposits with the Meridiani deposits suggests a common origin, though the mineralogy of the deposits across much of the region is obscured by dust. Thus it appears that the hydrological processes responsible for playa formation in Meridiani may have been active across much of the Arabia Terra region.

[6] Given the knowledge of the local environment at the time of deposition of the sedimentary sequence observed in Meridiani, the task remains to decipher the broader processes responsible for this environment and the implications for the climatic and hydrologic evolution of Mars. In a previous study, we used global hydrological models of a precipitation-evaporation- driven hydrological cycle to demonstrate that Meridiani Planum and the surrounding Arabia Terra region is a preferred locus for groundwater upwelling, driven primarily by the unique topography of Arabia Terra [*Andrews-Hanna et al.*, 2007]. We here use models of the global and regional scale groundwater hydrology to further investigate the distribution and behavior of water on Mars during the late Noachian and early Hesperian epochs. We build on the earlier study by considering the hydrological evolution at a higher spatial resolution, explicitly including the formation of evaporites and evaporite-cemented sedimentary deposits, and comparing the specific model predictions with the observed sedimentary record.

[7] The results demonstrate that the Meridiani playa deposits are the natural outcome of a precipitation-evaporation-driven hydrological cycle operating under warm but arid conditions on early Mars. The preserved deposits in Meridiani are predicted to be the remnant of a once larger deposit covering much of Arabia Terra, the vestiges of which are preserved elsewhere in the form of intracrater deposits, pedestal craters, and other deposits. Importantly, the hydrological cycle that drives the groundwater upwelling in Meridiani requires surface temperatures across the low to midlatitudes to have been above freezing for long periods of time, in order to facilitate both the precipitation-induced recharge of the low latitude aquifers and the groundwater evaporation upon reaching the surface. While the climate at the time was likely quite arid by terrestrial standards, the surface conditions would have been conducive to Earth-like life.

[8] The hydrological model and its implementation are described in section 2. Section 3 investigates the global hydrological cycle in the late Noachian to early Hesperian and the temporal evolution of groundwater flow and sedimentary deposition. Section 4 focuses on the regional hydrology of the Arabia Terra region. In section 5, the model predictions are compared with the observed sedimentary record of Arabia Terra. Alternative hypotheses for the origin of the deposits are discussed in light of the results and interpretations of this work in section 6. Finally, the implications for the early climate and history of water on Mars are discussed in section 7.

[9] In a companion paper (J. C. Andrews-Hanna, Early Mars hydrology: 2. Hydrologic, climatic, and geochemical evolution in the Noachian and Hesperian epochs, manuscript in preparation, 2010), we focus on the temporal evolution of the hydrological cycle from the Noachian through the early Hesperian. That paper places the Meridiani playa deposits within the broader context of the geomorphic and mineralogical evidence for the evolving climate of early Mars, focusing on the nature and cause of the phyllosilicate to sulfate deposition transition in the late Noachian [*Bibring et al.*, 2006].

2. Groundwater Model Description

[10] The early Martian hydrological cycle was likely driven by precipitation. While there has been much contention over how warm and wet early Mars was [e.g., *Squyres and Kasting*, 1994], some manner of precipitation-induced recharge would have been necessary to recharge the low-latitude aquifers in order to allow continued valley network formation [*Carr and Malin*, 2000; *Craddock and Howard*, 2002]. The question of whether this precipitation was in the form of liquid rain [*Craddock and Howard*, 2002] or snowfall that would then melt and percolate into the aquifers [*Carr and Head*, 2003] is of secondary importance to the resulting hydrological evolution. In either case, the precipitation would have recharged the low-latitude aquifers and, combined with the effects of the topography, would have driven groundwater flow down the local and regional hydraulic gradients. Under arid conditions, groundwater would flow through the aquifers until reaching the surface, at which point it would evaporate into the

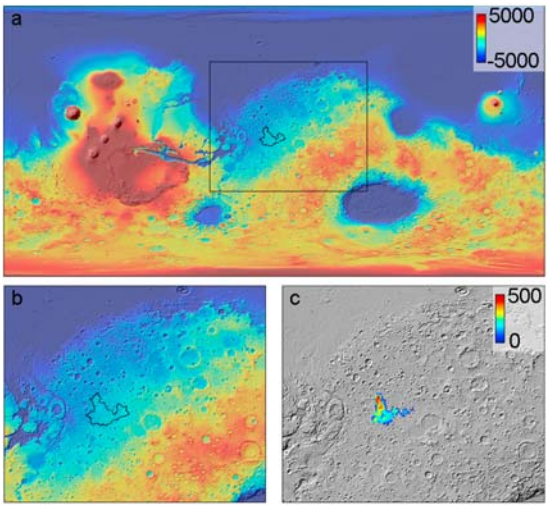

Figure 1. Topography in meters of (a) Mars (b) and Arabia Terra showing the location of the Meridiani deposits from *Hynek* [2004] (outline). (c) An approximation of the thickness of the deposits, calculated by interpolating the surrounding topography inward, was removed from the present-day topography prior to hydrological modeling.

atmosphere, only to be redistributed on the surface as precipitation and continue to cycle through the system.

[11] We represent the groundwater hydrology using a fully explicit finite difference model representing the equations of unconfined groundwater flow in a spherical shell grid:

$$\frac{\partial h}{\partial t} = \frac{1}{n}\left[\frac{1}{r^2 \sin^2\phi}\frac{\partial}{\partial\theta}\left(K \cdot d\frac{\partial h}{\partial\theta}\right) + \frac{1}{r^2 \sin\phi}\frac{\partial}{\partial\phi}\left(K \cdot d \cdot \sin\phi\frac{\partial h}{\partial\phi}\right) + s(\theta,\phi,t)\right] \quad (1)$$

where h is the hydraulic head (referenced to the geoid), K is the vertically averaged hydraulic conductivity (m/s), n is the aquifer porosity at the water table, d is the spatially varying height of the water table above the base of the aquifer (which is assumed to lie at a constant depth below the surface), s is a source term representing the influx from precipitation (m/s), r is the radius of the planet, θ is the longitude, φ is the colatitude, and t is time. The aquifer porosity and hydraulic conductivity are taken from the megaregolith model of *Hanna and Phillips* [2005]. The hydraulic conductivity is assigned to the vertically averaged value between the local water table and the base of the aquifer, and thus varies in both time and space during the simulations.

[12] Flow through the aquifer is driven by the gradients in the hydraulic head, which are established as a result of precipitation-induced recharge in the low latitudes and evaporative loss of groundwater in regions where the water table reaches the surface. Conditions on Mars in the late Noachian and early Hesperian are assumed to be arid, in agreement with the low erosion rates [*Golombek et al.*, 2006], low drainage densities, and immature state of the fluvial landscape [*Stepinski and Stepinski*, 2005; *Barnhart et al.*, 2009]. Thus, groundwater is assumed to evaporate upon reaching the surface, thereby limiting the water table to remain at or beneath the surface. The globally integrated evaporative loss of water in each time step is added back to the system in a low-latitude precipitation belt, with the relative latitudinal precipitation rate following a half cosine distribution between ± 45° latitude. This precipitation distribution is in first-order agreement with the observed distribution of valley networks. While the cause of the observed latitudinal limit on valley network formation is unknown, it is reasonable to suppose that the conditions that prevented high-latitude valley network formation likely inhibited aquifer recharge as well. Such conditions may entail either a lack of high latitude precipitation, or persistently cold high latitude temperatures that prevented the runoff and infiltration of precipitation.

[13] Models of groundwater flow on early Mars are limited by our ability to reconstruct the ancient surface topography. Tharsis appears to be an ancient feature [*Phillips et al.*, 2001], though it is unclear how much of Tharsis was in place at the time of sulfate deposition in the late Noachian to early Hesperian. Previous work considered the effect of removing the Tharsis load and induced deformation from the present-day topography and the hydrological effects of subsequent Tharsis formation [*Andrews-Hanna et al.*, 2007]. Prior to Tharsis formation, the lack of high elevation perched aquifers on Tharsis would have resulted in lower hydraulic heads on the periphery of the rise. During its formation, Tharsis may have acted as a hydrological sink due to the downward flexure of the lithosphere and burial of aquifers deep beneath the rise. After Tharsis formation, the expulsion of water from deeply buried aquifers may have acted as a hydrological source. However, that work found that the effect of Tharsis on the hydrology at Meridiani Planum and elsewhere outside of the rise was second order compared to the effects of the regional topography of the dichotomy, Arabia Terra, and the large impact basins [*Andrews-Hanna et al.*, 2007]. In this work, for the sake of simplicity, we do not remove Tharsis from the present-day topography.

[14] On a local scale, many of the craters on the surface today likely postdate the period of sulfate deposition, as evidenced by the presence of large craters both superimposed on and interbedded within the Meridiani deposits. The present-day topography includes both pristine unfilled craters and craters in various states of infill and exhumation [*Malin and Edgett*, 2000; *Edgett and Malin*, 2002]. While the specific short-wavelength topography of the surface today is not an exact representation of the topography of Mars in the late Noachian to early Hesperian, the early topography of Mars would not have differed dramatically in nature. Young craters on the surface today are similar in form to the young craters on the surface at the time of hydrological activity, while buried craters today do not affect the groundwater flow paths in the models.

[15] As the primary focus of this study is the origin of the Meridiani Planum sulfate deposits, we have removed a crude representation of the added topography of the deposits by interpolating the topography inward from the boundary of the etched terrain and contiguous plains units [*Hynek et al.*, 2002; *Hynek*, 2004] using an inverse distance to a power scheme (Figure 1). The subtracted layer thickness ranging from 0 to 450 m is conservative, as the Meridiani deposits are estimated to have a maximum thickness of ~600 m [*Hynek et al.*, 2002]. Outside of the etched terrain,

we initialize the models using the present-day geoid-referenced topography from MOLA [*Smith et al.*, 2001].

[16] Global models were run at a spatial resolution of 2.5 degrees per pixel, a limitation imposed by the model run times. These models are at a higher resolution than the 5 degrees per pixel results presented earlier [*Andrews-Hanna et al.*, 2007]. Higher resolution simulations were also performed locally at 0.25 degrees per pixel over a limited region, using the global model results as a boundary condition. Further details of the model implementation, benchmarking, and parameter sensitivity can be found in the appendices, including the effects of laterally heterogeneous aquifers and of different spatial distributions of precipitation on the surface.

3. Global Model Results: Evaporites and Sedimentary Deposits

3.1. Steady State Models

[17] We first consider the hydrological evolution of Mars during the late Noachian to early Hesperian using steady state models that neglect the modification of the surface that would be expected to result from an active hydrological cycle. Previous work found that the precipitation-evaporation-driven hydrological cycle operating under arid conditions led to the emergence of Meridiani Planum as a region of sustained groundwater upwelling and evaporation [*Andrews-Hanna et al.*, 2007]. We now look at the hydrology at a higher resolution of 2.5 degrees per pixel.

[18] The models are best characterized in terms of the initial mean water table depth implemented at the beginning of the simulation, which serves as a proxy for the total water inventory of the planet. We focus on models with an initial mean water table depth of 600 m, for which the predicted distribution of groundwater upwelling best matches the observed distribution of evaporites in Meridiani Planum. Rather than being a simple source of uncertainty, the initial mean water table depth is a parameter that would have experienced real variations over time during the early evolution of Mars. The total water inventory available to the hydrologic system would have been subject to both short and long-term forcing as a result of periodic changes in the surface temperature and volume of ice in the cryosphere driven by obliquity and orbital oscillations [*Laskar et al.*, 2004], and secular loss of water due to impact and solar wind erosion of the atmosphere [*Brain and Jakosky*, 1998]. The hydrological evolution for different assumed total water inventories, representing different stages in the hydrologic-climatic evolution of Mars, is examined in the companion paper (manuscript in preparation, 2010). In short, that work finds that the progression from valley network and phyllosilicate formation in the early to middle Noachian, to evaporitic sulfate deposition in the late Noachian to early Hesperian can be understood as a consequence of the effect that the changing global water inventory had on the evolving hydrological cycle. The declining total water inventory resulted in a decrease in precipitation rates, a deepening of the water table, and a focusing of groundwater upwelling within a few key regions of the planet, including Meridiani Planum and the surrounding Arabia Terra region. In this paper, we focus exclusively on the late Noachian to early Hesperian hydrology and the predicted distribution of evaporite deposits.

[19] For an initial mean water table depth of 600 m, the water table at hydrological equilibrium lies deep below the surface over most of the planet, including the majority of the midlatitude precipitation belt. The water table lies at or near the surface in a few isolated locations, including the interiors of the giant impact basins, areas north of the dichotomy boundary, the Valles Marineris canyon system, and Meridiani Planum and portions of the surrounding Arabia Terra region (Figure 2a). However, despite the broad regions of shallow groundwater, the water table only intersects the surface in a number of scattered points, generally corresponding to the deepest craters and other depressions in regions with a shallow water table (Figures 2a and 2b). The effect of these local topographic lows in the steady state models partially masks the long-wavelength regional distribution of groundwater upwelling found in the earlier lower resolution models [*Andrews-Hanna et al.*, 2007], though some concentration of loci of groundwater upwelling is observed in Arabia Terra. The regional groundwater upwelling throughout Arabia Terra only becomes apparent in models that include active sedimentary deposition, as shown in the next section.

3.2. Dynamic Models: Effects of Sedimentary Deposition

[20] The simplistic steady state model above provided a static snapshot of the inherently dynamic hydrological evolution of the planet. As a result of the arid climate assumed in the models, groundwater reaching the surface will evaporate and leave behind any dissolved solutes in the form of evaporite deposits and evaporite-cemented sediments. As aeolian material is transported across the surface, it will be infiltrated by the rising groundwater table and indurated into an erosion-resistant deposit. The resulting deposits may range from pure evaporitic salts to weakly cemented sand and dust. The isolated topographic lows that intersect the water table will fill with sediments, allowing the water table in the surrounding area to rise toward the surface. The result is a dynamic hydrologic system in which the patterns of groundwater flow and evaporation alter the surface topography, which in turn affects the groundwater flow.

[21] This infilling of local topographic lows can result in one of two outcomes, depending on the hydrologic environment: either the depression will partially fill with sediments until the water table ceases to rise and the flux of groundwater to the surface terminates, or the depression will completely fill with sediments and the rising water table will intersect the surface throughout the surrounding area. A similar process to the first scenario may have occurred on a much smaller scale after the impact that formed Meteor Crater in Arizona, in which the excavated crater penetrated to below the paleo water table leading to ancient lake and playa deposits on the crater floor [*Kring*, 2007]. The sedimentary infilling of Martian craters is supported by observations of layered sedimentary deposits within many craters [*Malin and Edgett*, 2000], as discussed further in section 5. By smoothing out the short-wavelength topographic lows, the earlier low-resolution models approximated the hydrology of the planet in a more evolved state, after substantial sedimentary infilling of the topographic lows.

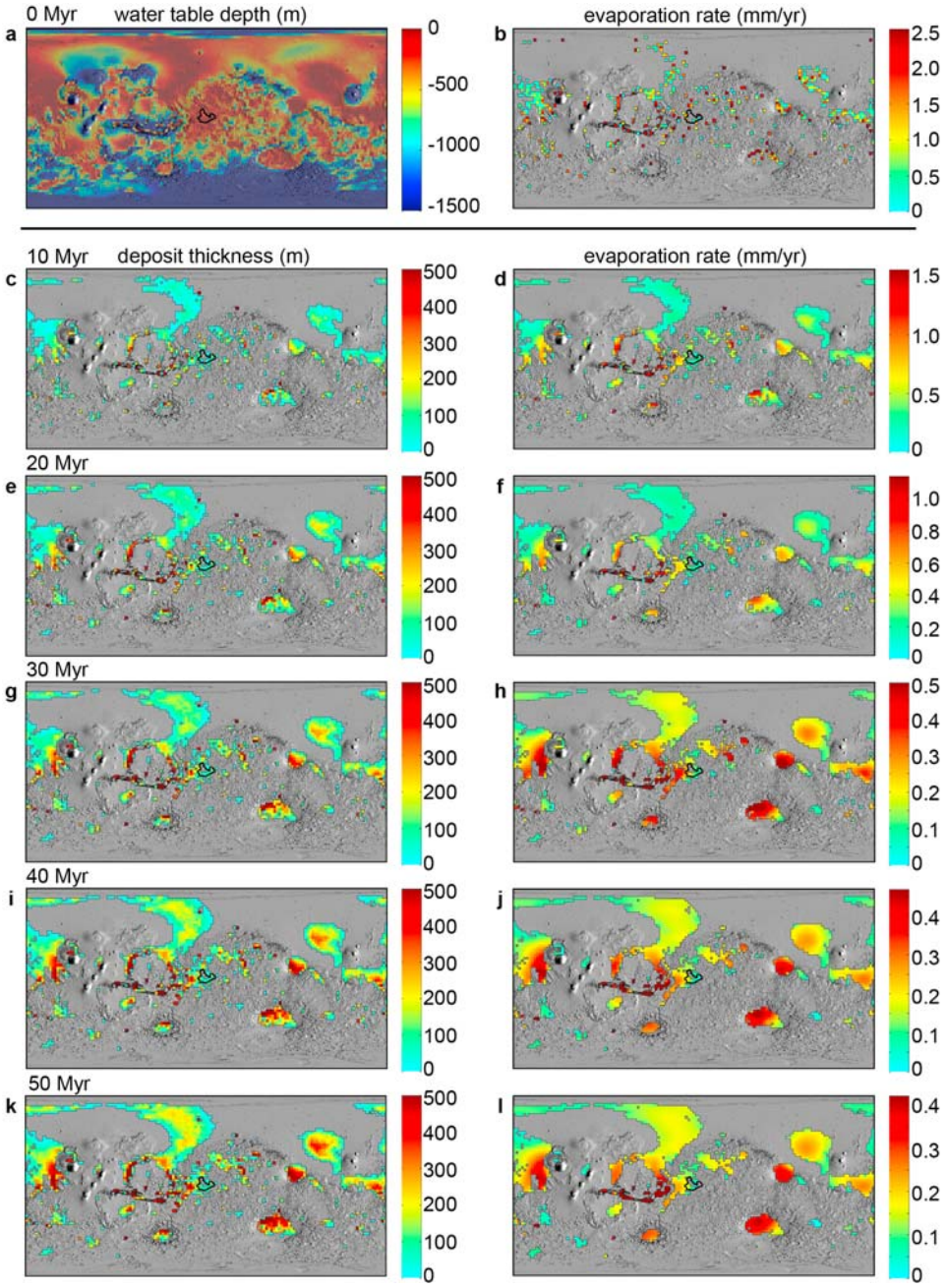

Figure 2. Time evolution of the global hydrological model over 50 Myr. (a) The depth to the water table varies little from its initial state. (b) The groundwater upwelling and evaporation is initially restricted to the deepest craters and low points. (c, e, g, i, and k) Over the course of the 50 Myr simulation, the deposits thicken and spread out over the surface while (d, f, h, j, and l) the rate of groundwater upwelling decreases. The location of Meridiani Planum and the surrounding etched terrain are outlined in each plot.

[22] In order to better represent the hydrologic evolution of Mars, we now incorporate deposition of evaporites and cemented sediments into the models. The water reaching the surface at Meridiani and elsewhere has flowed underground at depths of up to a kilometer for distances of up to thousands of kilometers, with flow timescales on the order of millions of years. Thus, there is ample time for these fluids to equilibrate with the aquifer matrix. Comparable ancient fluids from deep drill holes on the Earth can have salinities exceeding that of seawater [*Moller et al.*, 1997], though the salinity will be strongly affected by the host rock lithology and the duration and temperature of water-rock interaction. The mineralogy of the Meridiani deposits suggests that the fluids at the surface possessed higher solute concentrations and lower water activities than terrestrial seawater [*Tosca et al.*, 2008], though these salinities may reflect the fluid composition after substantial evaporitic concentration. We assume that the deep groundwater has a salinity equal to 80% that of seawater upon reaching the surface [e.g., *Handford*, 1991], and that the deposits incor-

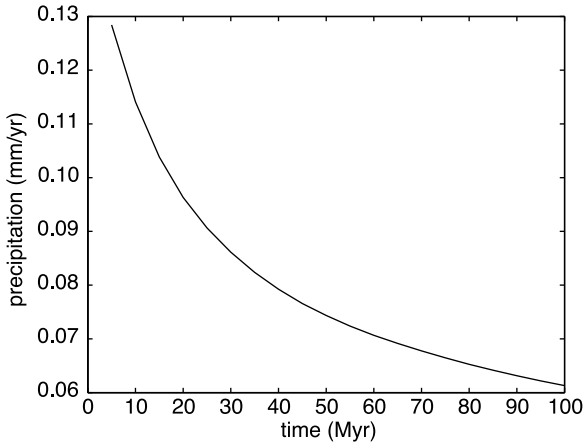

Figure 3. Evolution of the equatorial precipitation rate during a global simulation. The precipitation distribution follows a cosine function between ± 45° latitude, with the rate set such that globally integrated precipitation exactly balances the globally integrated outflow and evaporation from the aquifers.

porate 50% by volume of clastic sediments based on mini-TES observations at Meridiani [*Glotch and Bandfield*, 2006] and similar to other "dirty" evaporites in playa settings, such that evaporation of 100 m of groundwater produces 2 m of evaporitic sediments. The hydrologic system evolves slowly in a state of quasi-equilibrium with the changing surface topography, so different fluid salinities or clastic fractions can be represented by simply scaling the model timescale. Meteoric rainwater is assumed to have a negligible concentration of dissolved solutes, so any direct meteoric contribution to the local evaporation flux does not result in evaporite deposition. The added sedimentary deposits are assumed to have identical hydraulic properties to the underlying aquifers.

[23] The models are first run without evaporite deposition for 100 Myr to attain hydrological equilibrium, and then for an additional 100 Myr during which the topography is updated to reflect evaporite deposition. When evaporite deposition is explicitly included in the models, the isolated craters and depressions in which the groundwater upwelling was initially concentrated rapidly fill with evaporites. After 10 Myr, many of the initial loci of groundwater evaporation are deactivated due to sedimentary infilling (Figures 2c and 2d). In a few locations, sedimentary infilling of the local topographic lows is accompanied by regional groundwater rise, leading to broad regions of more evenly distributed groundwater evaporation. The distribution of groundwater evaporation across the surface becomes dominated by the long-wavelength patterns of groundwater flow, similar to the low-resolution hydrological models of *Andrews-Hanna et al.* [2007]. After 50 Myr, large-scale evaporite deposits in excess of several hundred meters thickness are found in several locations in the northern lowlands, within the large impact basins, in the Valles Marineris canyons, and concentrated in Meridiani Planum and the surrounding Arabia Terra region (Figure 2k). The smoothing of the topographic lows has a diffusive effect on the distribution of groundwater upwelling, leading to broad regions of smoothly varying groundwater flux (Figure 2l). While the distribution of groundwater upwelling changes dramatically over the course of the simulation, the long wavelength shape of the water table is largely unaffected, since the actual changes to the surface topography are small.

[24] As found in the earlier study, Meridiani Planum is one of the few regions of presently exposed Noachian-aged crust for which a sustained flux of groundwater upwelling and evaporation is predicted. *Andrews-Hanna et al.* [2007] showed that the groundwater upwelling in Meridiani is driven predominantly by the regional slopes of the Arabia Terra region. For the simple case of steady one-dimensional flow, conservation of water volume results in an inverse relationship between the topographic slope and height of the water table relative to the surface, leading to a relative rise in the water table accompanying a transition from steep to gentle slopes. Arabia Terra is a unique region of Mars, intermediate between the highlands and lowlands in crustal thickness and topography, and separated from each by distinct breaks in slope along its northern and southern boundaries (Figures 1a and 1b). The location of Meridiani Planum just below the break in slope leading down into Arabia Terra from the highlands results in a rise of the water table to the surface. This effect allows for a sustained flux of groundwater to the surface at Meridiani, despite its location along a sloping surface rather than within a confined basin.

[25] Predicted evaporite deposits in the northern lowlands and large impact basins would likely have been buried beneath subsequent volcanic and sedimentary deposits. Evaporite deposits are also predicted within the Valles Marineris canyons and in the nearby chaos regions and outflow channels, though it is uncertain to what extent these topographic lows had developed by the late Noachian to early Hesperian. This result agrees well with the detection of sulfates both in the Valles Marineris layered deposits [*Griffes et al.*, 2007; *Murchie et al.*, 2009] and in layered deposits within Aram and other chaos regions [*Glotch and Christensen*, 2005; *Glotch and Rogers*, 2007; *Noe Dobrea et al.*, 2008], and with the common association of hematite with these deposits [*Christensen et al.*, 2000; *Glotch and Christensen*, 2005]. Regional hydrological models have been used to investigate the groundwater flux and sedimentary filling of Candor Chasma [*Murchie et al.*, 2009]. The local depositional environments in different settings may have ranged between lake, playa, spring mound, and soil cementing deposits, leading to the observed morphological diversity. However, we suggest that the underlying causes behind these widely separated sulfate deposits in differing depositional settings are the same: long-wavelength deep groundwater flow induced by a precipitation-evaporation-driven hydrological cycle interacting with the surface topography.

[26] Prior to evaporite deposition, the equatorial precipitation rate in balance with the globally integrated evaporation rate in the model is 1.55×10^{-4} m/year, and the mean groundwater flux at Meridiani is 1.43×10^{-4} m/year. As sedimentary deposition fills in the local topographic lows, the mean path length of groundwater flow increases. This increases the residence time of water in the subsurface, thereby decreasing the rate of water cycling between the aquifers and atmosphere, and decreasing the precipitation rate (Figure 3). After 50 Myr, the equatorial precipitation rate is only 7.43×10^{-5} m/year, and the groundwater flux at

Meridiani is 2.56×10^{-5} m/year. Although the precipitation rate at Meridiani exceeds the groundwater flux to the surface, the groundwater would have carried a high solute concentration in comparison to the dilute meteoric water. While constraints on the deposition rate at Meridiani are lacking, we show in section 5 that the predicted deposition rate at Becquerel crater matches that inferred from a comparison of the layer periodicity with the obliquity evolution of Mars [*Lewis et al.*, 2008]. The predicted slow migration of fluids through the crust at Meridiani is consistent with the stagnant aquifer conditions inferred from the small size and near-spherical shape of the hematite concretions observed by the Opportunity rover [*McLennan et al.*, 2005; *Sefton-Nash and Catling*, 2008].

[27] The specific rates of precipitation and evaporation early in the simulations are sensitive to the model resolution. The precipitation rate in the models balances the globally integrated evaporation rate, and thus provides a measure of the rate of water cycling through the hydrologic system. At higher resolutions, shorter wavelength craters and depressions are resolved in regions of shallow water table. As a result, the mean path length of groundwater flow decreases, and the net rate of water cycling and the precipitation rate increase. The equatorial precipitation rate for global models with grid resolutions of 2.5 to 0.25 degrees per pixel ranges from 1.55×10^{-4} to 4.0×10^{-3} m/year. However, the model resolution has little effect on the regional patterns of groundwater flow or the depth to the water table. As the high resolution models evolve, the sedimentary infilling of the topographic lows increases the flow path lengths, the precipitation rates decrease, and the results converge with those of the lower resolution models.

[28] The low predicted precipitation rates are consistent with the lack of evidence for modification of the deposits by dilute meteoric water. Comparable mean precipitation rates are observed locally in hyperarid regions on the Earth, including portions of the Atacama Desert of Chile that receive less than 1 mm of rainfall per year on average with significant interannual variability [*Houston*, 2006]. The predicted rates of groundwater upwelling and midlatitude precipitation should be considered to be long-term averaged rates. In reality, Mars would have experienced climatic and hydrological perturbations that would have modulated these average rates. The predicted low precipitation rates may translate into long periods of hyperaridity punctuated by occasional climatic optima due to orbital forcing [*Laskar et al.*, 2004], in which the climate was similar to arid or semiarid environments on the Earth [*Barnhart et al.*, 2009]. Similarly, the continued impact bombardment of the surface would have resulted in repeated perturbations to the hydrologic cycle on a local to regional scale, with a large fresh impact crater lowering the water table and inhibiting groundwater upwelling over a broad region, until sufficient sedimentary infilling of that crater allowed the regional water table to again intersect the surface.

4. Regional Models: Arabia Terra and Meridiani Planum

[29] The resolution of the global models is limited by the computational time required. However, it is possible to investigate the hydrology of particular regions at higher resolution by embedding regional hydrological models within the results of the global models. This approach is similar to that taken by *Harrison and Grimm* [2008] in studying the outflow channels. The hydraulic head from the global models is used as a constant head boundary condition around the periphery of the region of interest. The resolution of the steady state global model was first refined from 2.5 to 1.25, and finally to 0.25 degrees per pixel, using the coarser resolution model results as the initial condition in the successively higher resolution models, allowing rapid equilibration at the higher resolutions. The results of the high resolution steady state global model are then used as the initial condition and boundary conditions of a local dynamic model encompassing the region of interest, in order to track the history of groundwater flow and evaporite deposition over longer periods of time.

[30] Applying constant head boundary conditions to the local model neglects the small changes in topography and hydraulic head that should occur due to sedimentation beyond the margins of the region, but this has little affect on the evolution away from the boundaries. The precipitation rates must be dictated by the condition of global conservation of water volume, and will change as evaporite deposition alters the mean path length and net rate of groundwater cycling. The local models cannot track global water conservation, so we instead apply the time-evolving precipitation rates from the lower resolution dynamic global models. This will underestimate the precipitation and evaporation rates early in the simulation, but have little effect as the system evolves, other than to increase the time required to generate deposits of a given thickness in these local models relative to the global models.

[31] The evolution of the local height of the water table in Meridiani Planum and the surrounding Arabia Terra region is determined primarily by recharge within the highlands to the south and evaporation in the lowlands to the north [*Andrews-Hanna et al.*, 2007], thereby dictating that the regional model extend beyond the northern and southern edges of Arabia Terra. We define a rectangular region of interest in latitude-longitude space enclosing Arabia Terra and including a portion of the adjacent highlands and lowlands (Figure 4b). As in the global models, the Meridiani hematite unit and etched terrain have been subtracted from the topography. We have similarly filled in the depressions of the large outflow channels in the western portion of the region, though these do not strongly affect the groundwater flow in the rest of the region.

[32] Early in the simulation, evaporite formation is restricted to scattered impact craters and other topographic lows, which are now resolved down to a scale of 10s of km. However, even at this early stage it is clear that the region encompassing Meridiani Planum exhibits a particularly shallow water table (Figure 4a). As the system evolves, the deepest depressions are filled with sediments, allowing the water table to rise toward the surface over much of Arabia Terra (Figures 4d, 4g, 4j, and 4m), leading to broadly distributed sedimentary deposits (Figures 4e, 4h, 4k, and 4n) and large areas of nearly uniform groundwater upwelling (Figures 4f, 4i, 4l, and 4o). Looking at the distribution of evaporites after 200 Myr (Figure 4n), we find two classes of deposits. Local deposits with thicknesses of up to 1 km are found within many of the closed depressions, including the

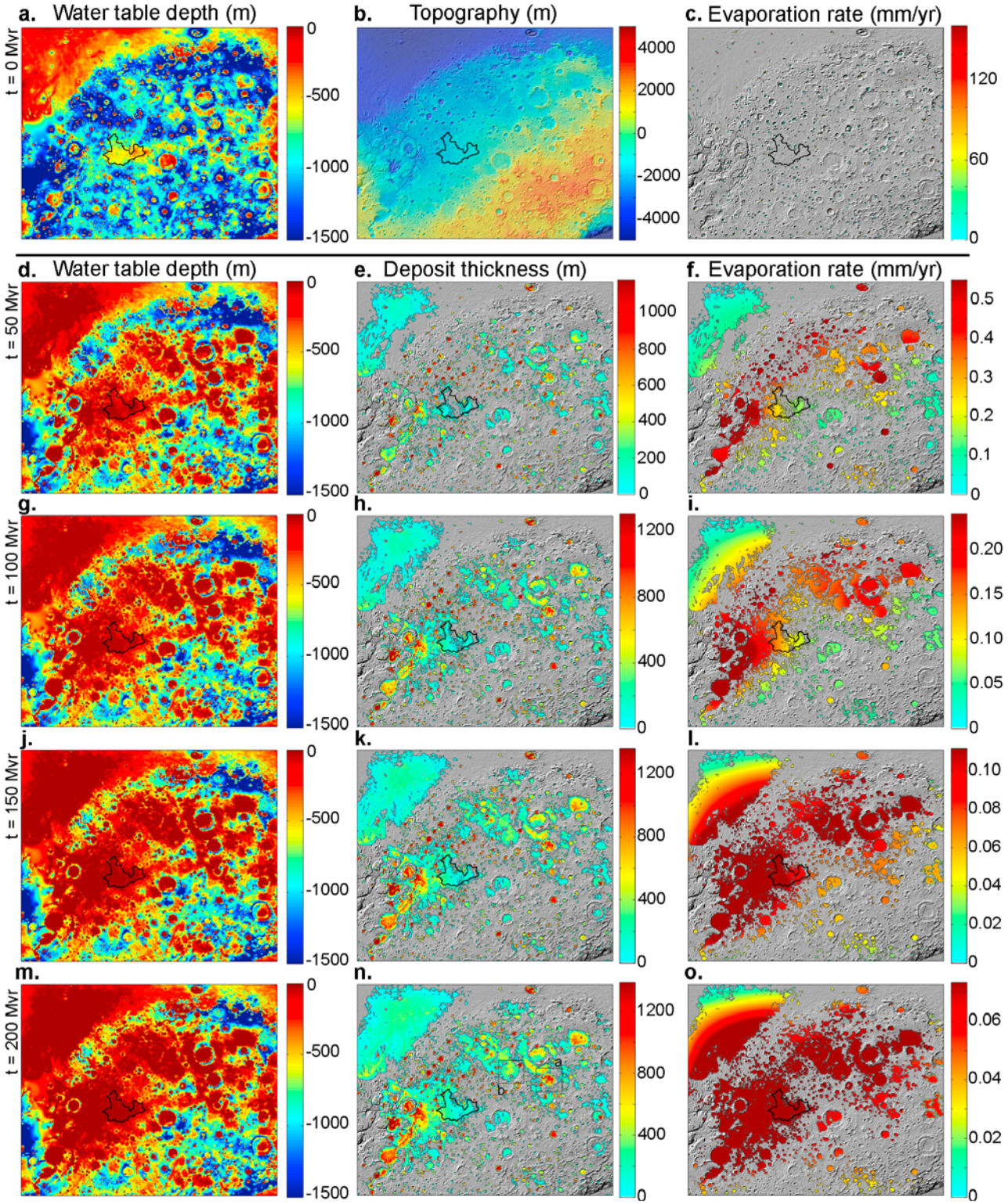

Figure 4. (a) The depth to the water table, (b) topography (with the Meridiani etched terrain and major outflow channels removed), and (c) groundwater upwelling rate and distribution (with groundwater upwelling restricted to isolated model pixels at t = 0 Myr) are shown at the initiation of the local hydrological model of Arabia Terra. (d, g, j, and m) As the model evolves, the water table rises toward the surface throughout the region, (e, h, k, and n) the deposits thicken and spread over the surface, and (f, i, l, and o) the groundwater upwelling and evaporation rate spreads over the surface and decreases in magnitude. All model results are superimposed over MOLA shaded relief. Boxes in Figure 4n show the locations of Figures 9a and 9b.

large impact craters and the chaos regions in western Arabia Terra. Extensive evaporite deposits are also found spreading out over the intercrater plains, particularly in the vicinity of Meridiani Planum, that are not contained within closed topographic depressions. After 200 Myr, the deposits in Meridiani have reached a maximum thickness of 850 m and mean thickness of 120 m, comparable to the thickness of the deposits removed from the original topography (450 m and 180 m, respectively).

[33] The fact that the observed deposits are more limited in lateral extent, and yet thicker on average and with steeper margins than predicted by the models, suggests that they are the end product of a combination of primary evaporite/playa deposition and secondary erosion and redeposition, consistent with the in situ observations by Opportunity. A key example of this secondary modification of the original deposits is found in Miyamoto crater at the southwest edge of the Meridiani deposits. *Wiseman et al.* [2008] showed that the ancient phyllosilicate-bearing Noachian floor is exposed in the southwest corner of the crater, immediately adjacent to thick stacks of sulfates in the northeast portion of the crater. That study argued that the deposits once filled the crater and were later eroded back to their present extent. The groundwater models predict that evaporite deposition should have been active throughout the crater floor, with peak rates in the southwest portion of the crater. The steep margin of the deposits filling the northeast portion of the crater cannot be explained by hydrological processes alone, since a water table controlled by diffusive flow will assume a more gradual profile. Erosion and redeposition of the sulfates could have occurred either during or after the initial deposition.

[34] The model predictions are consistent with the observed continuity of layers over distances of 100s of km within Meridiani and the low dip angles that generally conform to the regional topography [*Hynek and Phillips*, 2008]. After the infill of the large craters in the region, the water table is predicted to follow a smoothed version of the surface topography. As the system evolves, broad regions of relatively uniform groundwater evaporation are predicted over much of Arabia Terra (Figure 4o). This would gradually build up large-scale deposits with coherent layering over long distances through either direct evaporite deposition or the cementation of aeolian deposits. *Hynek and Phillips* [2008] find layer dips clustered between 0.05° and 1.0°, with dip azimuths between −15° and −60° measured clockwise from north. Considering the predicted deposit surface (representing the primary bedding plains) within the Meridiani etched terrain, we find dip azimuths of −46 ± 18° and dips of 0.035 ± 0.008°. While the predicted dip azimuths agree well with the observations, the predicted layer dips are on the low end of the measured range. The somewhat greater observed layer dips may be a result of either postdepositional deformation or increased hydraulic gradients resulting from spatial variations in either the aquifer properties or the distribution of precipitation.

[35] In simulations in which the precipitation rate was arbitrarily terminated, the groundwater flux at Meridiani ceased within 5 Myr. This brief period of continued groundwater discharge after the termination of the precipitation-induced recharge is insufficient to generate the observed thickness of the deposits. Thus, despite the fact that none of the direct morphological observations on the surface in Meridiani require active precipitation, maintenance of the hydrological environment responsible for the playa deposits requires continued low-latitude precipitation on Mars as late as the early Hesperian.

5. Comparison With the Sedimentary Record of Arabia Terra

[36] The hydrological models highlight Arabia Terra as a region of enhanced groundwater upwelling early in Mars history, and predict that widespread evaporite-cemented sedimentary deposits should have formed across much of this region. While direct evidence for playa evaporites from in situ observations exists only at one location in Meridiani Planum, there is abundant evidence for sedimentation and hydrological activity throughout Arabia Terra.

[37] One of the key predictions of the models is that the large craters and other topographic lows in Arabia Terra should have been filled with evaporites and cemented sediments prior to playa development at Meridiani. MOLA topography reveals a number of large, mound-like sedimentary deposits within craters (Figure 5). These deposits exhibit thicknesses of up to 2 km. The deposits in Crommelin crater (Figures 5b and 5i) exceed the elevation of the crater rim, suggesting that the deposits at one time filled the crater and covered the surrounding Noachian plains. This is supported by the observation of pedestal craters outside of Crommelin that reach a similar peak elevation to the intracrater deposit, which further suggests that the majority of the deposits in Crommelin lie stratigraphically below the deposits on the surrounding intercrater plains. Distinct topographic benches in the deposits within Henry crater suggest layers with varying degrees of induration (Figures 5c and 5j), possibly modulated by perturbations to the climatic-hydrologic system during deposition. That the deposits at one time filled the craters rather than having formed with their current mound morphologies is evidenced by the presence of a topographic bench along the wall of Becquerel crater at the same elevation as the intracrater mound (Figures 5d and 5k).

[38] The presence of thick layered deposits within craters lacking any obvious fluvial input is strongly suggestive of a groundwater source, and previous studies have interpreted these and other light-toned layered deposits as large-scale spring deposits [*Rossi et al.*, 2008]. Many craters within Arabia Terra exhibit varying states of fill and exhumation [*Malin and Edgett*, 2000], suggesting that the observed extent of sedimentary deposits may belie their original distribution. Some craters lacking deposits may have been filled and then fully exhumed, while others may postdate the main period of groundwater upwelling and evaporite deposition.

[39] For the deposits within Becquerel Crater, high resolution images and DEM's have allowed a direct correlation of the observed layer bundling with the predicted obliquity cycle of Mars, leading to a calculated deposition rate of 3×10^{-5} m/year [*Lewis et al.*, 2008]. This deposition rate is in excellent agreement with the predictions of the local model for Becquerel of a groundwater upwelling rate of 10^{-3} m/year and deposition rate of 2×10^{-5} m/year early in the simulation (Figure 4f). While the predicted deposition

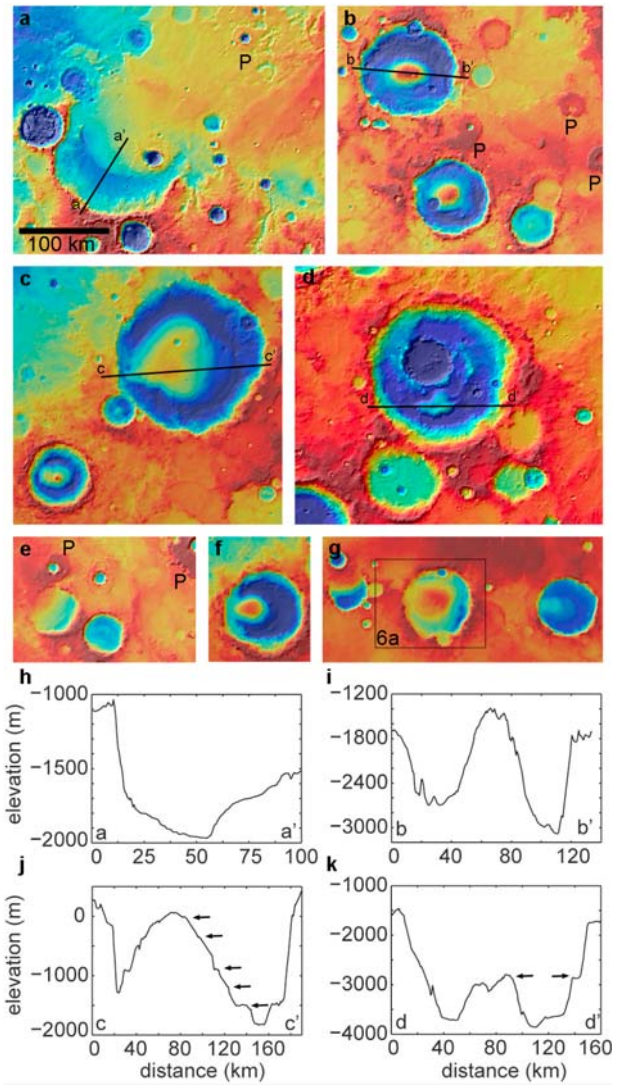

Figure 5. MOLA topography of select large intracrater deposits, including (a) Miyamoto, (b) Crommelin, (c) Henry, (d) Becquerel, (e) Vernal crater, (f) a crater near Tuscaloosa crater, and (g) craters near Capen which is crater on right. The presence of pedestal craters ("P") on the surrounding intercrater plains suggest that deposits may have once been more laterally extensive. Topographic profiles of (h) Miyamoto, (i) Crommelin, (j) Henry, and (k) Bequerel reveal the thickness of the deposits. Topographic steps in Henry (Figure 5j, arrows) suggest large-scale internal layering. A bench in the wall of Becquerel at the same elevation as the intracrater deposit (Figure 5k, arrows) suggest that the deposits at one time filled the entire crater. The box in Figure 5g reveals the location of the CRISM parameter map in Figure 6a.

rate is highly sensitive to the poorly constrained aquifer hydraulic conductivity and the assumed ratio between the deposit thickness and the evaporated water column, the close agreement of the predicted and observationally inferred rates lends strong support to the interpretation that these intracrater deposits formed as a result of groundwater inflow.

[40] The composition of the intracrater deposits is masked by dust across much of the region, as evidenced by the low thermal inertia derived from TES [*Putzig et al.*, 2005]. However, the Arabia Terra region as a whole is an area of enhanced hydration, as observed by the gamma ray and neutron spectrometer aboard Mars Odyssey [*Boynton et al.*, 2002; *Feldman et al.*, 2004]. This broad, diffuse signature of enhanced hydration may reflect the presence of both the hydrated sulfate deposits and the redistributed erosional debris from the deposits. In some locations, spectral signatures indicative of the presence of hydrated sulfates are observed in CRISM observations of the intracrater deposits. A hydrated sulfate parameter map was constructed from CRISM multispectral (MSP) data over part of Arabia Terra (using the D2100, D2400, and D1900 band depth parameters from *Wiseman et al.* [2010], similar to those of *Pelkey et al.* [2007]). Hydrated sulfate identifications are found associated with a number of large intracrater deposits, including one in southern Arabia Terra ~300 km from the edge of the Meridiani etched terrain (Figure 6). Absorption features near 1.9 and 2.4 μm indicate the presence of polyhydrated sulfates [*Cloutis et al.*, 2006]. The strongest sulfate detections in this case are at the bottom of a partially exhumed deposit, which may be due to a greater sulfate concentration or difference in sulfate mineralogy lower in the deposits. This would be consistent with the model prediction of a decreasing groundwater influx as the craters fill with sediment, which would result in a higher evaporite to clastic ratio lower in the stratigraphic section.

[41] A survey of large craters (>100 km diameter) across Mars reveals a distinct concentration of intracrater sedimentary deposits in Arabia Terra (Figure 7a). Similarly, in a study of open crater lakes, *Fassett and Head* [2008] used the size of the upstream drainage basins to evaluate the relative importance of runoff versus groundwater inflow. They found that the open lake basins inferred to have experienced a greater contribution from groundwater inflow were concentrated primarily in Arabia Terra (Figure 7b). This is consistent with the predicted shallow water table and elevated ratio of groundwater flux to precipitation predicted throughout the region.

[42] The sulfate-hematite deposits within Aram chaos represent an interesting and unique case of an intracrater deposit [*Christensen et al.*, 2000; *Gendrin et al.*, 2005; *Glotch and Christensen*, 2005; *Lichtenberg et al.*, 2010]. Aram crater lies in the westernmost portion of Arabia Terra, and hosts a chaos region that contributed to the flow within Ares Vallis. Spectral data reveal a km thick sulfate and hematite deposit that is stratigraphically above the chaos on the crater floor. This intracrater deposit postdates the Meridiani deposit by up to 1 Gyr [*Glotch and Christensen*, 2005], yet exhibits striking mineralogical and morphological similarities [*Glotch and Christensen*, 2005; *Lichtenberg et al.*, 2010]. While the relationship between the intracrater deposit and the chaos in Aram provide a strong link between the Arabia Terra intracrater deposits and groundwater upwelling, the timing of evaporite deposition presents a conundrum. Chaos formation and outflow flooding are commonly thought to require cold climate conditions and a thick cryosphere, while the playa hypothesis for the origin of the Meridiani deposits requires evaporating liquid water at or near the surface. The sequence in Aram could be in-

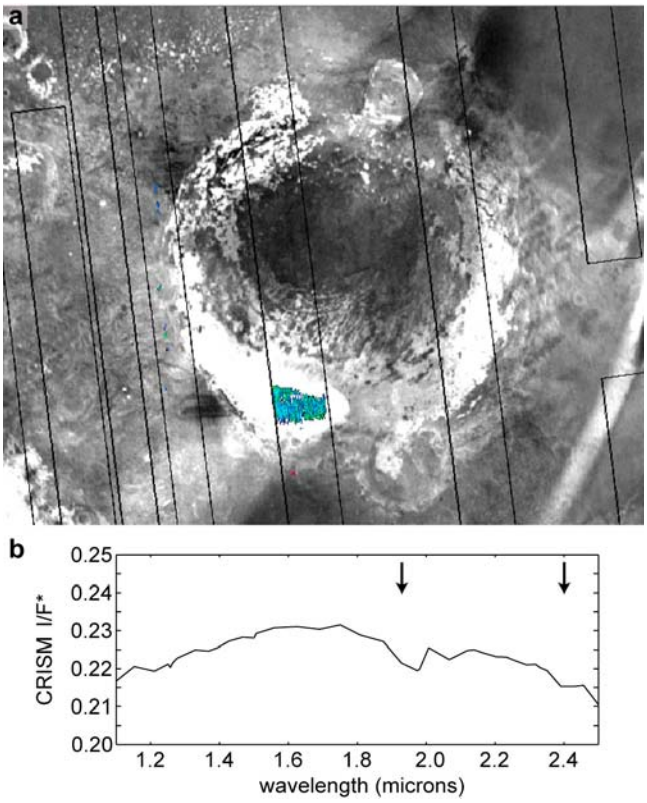

Figure 6. CRISM hydrated sulfate parameter map over a large intracrater deposit (see Figure 5g for context), created from volcano scan-corrected CRISM I/F multispectral data (a) R, D2100; G, 2400; B, D1900, similar to the spectral parameters of *Pelkey et al.* [2007] superimposed over a THEMIS NIR mosaic also showing the CRISM MSP coverage. In this color scheme, polyhydrated sulfates are represented as cyan and monohydrated sulfates as yellow (not identified). (b) The spectrum reveals absorption features at 1.9 and 2.4 μm, consistent with the identification of polyhydrated sulfates. Brighter tones in the THEMIS NIR base map indicate surface materials with a greater degree of induration or larger grain size.

terpreted either as a result of a significant climatic swing to warm conditions in the late Hesperian after outflow channel formation or, more likely, as a result of local conditions within Aram that permitted a depositional environment similar to that in Meridiani despite the prevailing cold climate [*Glotch and Christensen*, 2005]. Hydrological models of outflow channel floods from chaos regions demonstrate that the late stage fluids originate from the deepest portions of the aquifer [*Andrews-Hanna and Phillips*, 2007], suggesting the possibility of a flux of warm deep brines to the surface and a hydrothermally enhanced heat flux. If evaporation of these upwelling brines outpaced freezing, a playa-like deposit similar to that in Meridiani may result even under cold climate conditions. This process would have been aided by the freezing point depression resulting from evaporitic concentration of the salts in the near-surface fluids. The widespread abundance of older intracrater deposits across Arabia Terra coupled with the predictions of the hydrological models argue that substantial sulfate deposits would also have formed within Aram crater prior to chaos formation and outflow flooding. This original intracrater deposit would have been disrupted and reworked by the emerging flood waters, and ultimately carried downstream in the flood and/or redeposited in the crater lake above the chaos.

[43] In addition to the sedimentary infilling of large craters, other topographic lows should have been preferentially filled with evaporite-cemented materials. Fluvial valleys, by nature, follow local topographic lows. If the valley networks received any significant fraction of their flow from groundwater, as is commonly the case on Earth, they would represent locations in which the surface topography intersected the paleo water table during periods of active formation. After the transition to a more arid hydrologic-climatic

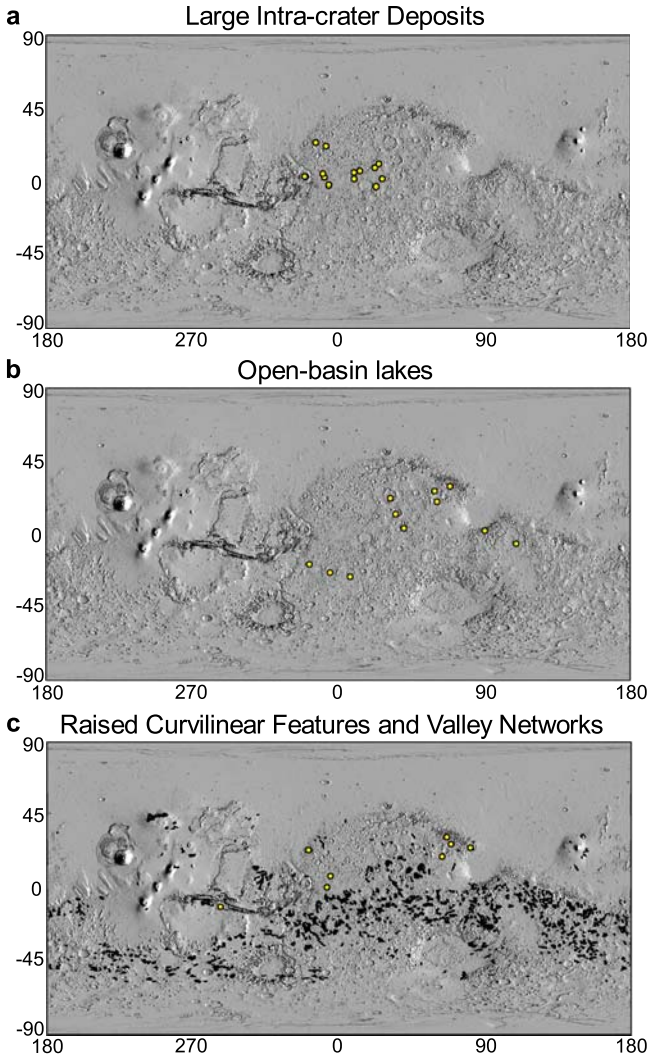

Figure 7. Evidence of hydrological activity and deposition in Arabia Terra, including (a) the distribution of large intracrater deposits, (b) the concentration of open basin lakes showing evidence for a substantial groundwater contribution (from *Fassett and Head* [2008]), and (c) the concentration of raised curvilinear features representing inverted valley networks (valley networks represented in black from *Carr and Chuang* [1997]; raised curvilinear features represented by circles from *Williams* [2007]).

regime in the late Noachian (manuscript in preparation, 2010), the valley networks in Arabia Terra would be preferred locations for evaporite deposition. While Arabia Terra exhibits a lower density of valley networks than the rest of the equatorial southern highlands [*Carr and Chuang*, 1997], there is a significant concentration of inverted valley networks in the region [*Fassett and Head*, 2007; *Williams*, 2007] (Figure 7c). The topographic inversion of these valleys is most easily explained by the valleys having been filled with an erosion-resistant indurated material, and then left as high-standing ridges when the surrounding terrain later experienced net deflation or erosion.

[44] As discussed in the companion paper (manuscript in preparation, 2010), the transition to arid conditions over most of the surface of Mars would cause the water table to drop deeper beneath the surface, arresting the development of fluvial features. In Arabia Terra, the water table would have remained close to the surface into the Hesperian. During this transition, valley networks in Arabia Terra would see a dramatic decrease in the total flux of water, an increase in the ratio of groundwater- to precipitation-sourced fluids, and a concomitant increase in the fluid salinity. The channels would experience a transition from high discharge erosional flow to low discharge seepage and evaporation, leading to either evaporite deposition or cementation of aeolian debris. While inverted valley networks can be produced by a number of mechanisms, the concentration in Arabia Terra is consistent with valley infill by evaporites and cemented sediments due to the regional groundwater upwelling in Arabia Terra, followed by net deflation of the surrounding surface.

[45] Beyond Meridiani, a widespread mantling unit mapped throughout Arabia Terra [*Greeley and Guest*, 1987] has been attributed to an origin as a paleo polar layered deposit [*Schultz and Lutz*, 1988; *Niles and Michalski*, 2009], or through aeolian, sedimentary, or volcanic processes [*Grant and Schultz*, 1990; *Moore*, 1990; *Fassett and Head*, 2007]. MOC images reveal meter-scale layering, interpreted as evidence for water-lain sedimentary rocks [*Malin and Edgett*, 2000; *Edgett and Malin*, 2002]. The morphology, layering, and relief of the mantling units in eastern Arabia suggest deposits of dust to sand-sized particles of aeolian or air fall origin, exhibiting variable degrees of induration or cementation, leading to inverted topography of craters and valleys [*Fassett and Head*, 2007]. A reasonable chain of inference connects the widespread deposits across Arabia Terra with those in Meridiani. Correlation of the stratigraphic section observed by Opportunity with a widespread light toned, high thermal inertia, etched unit in western Arabia Terra suggests that at least these deposits are genetically related to the playa deposits observed in Meridiani [*Hynek*, 2004]. OMEGA and CRISM spectra confirm the presence of sulfates in dust-free western Arabia Terra [*Gendrin et al.*, 2005; *Griffes et al.*, 2007; *Poulet et al.*, 2008; *Wiseman et al.*, 2010], and similar indurated deposits are seen throughout the region. The large intracrater deposits across Arabia Terra are morphologically similar to the intracrater deposit in Miyamoto crater (Figure 5a), which is directly continuous with the Meridiani plains. Intracrater deposits in the vicinity of Meridiani Planum have been identified as outliers of the etched terrain [*Hynek*, 2004].

[46] These deposits have experienced significant erosion since their initial deposition, as evidenced by erosional surfaces cutting across the bedding, craters in varying states of fill and exhumation [*Malin and Edgett*, 2000], and erosional outliers surrounding the Meridiani deposits [*Hynek*, 2004]. Pedestal craters are common throughout Arabia Terra, formed when ejecta from impact craters armored friable sedimentary deposits, such that subsequent erosion and deflation of the surface left the crater ejecta blanket as a high-standing plateau. Pedestal craters similar to those seen elsewhere in Arabia Terra are seen both beyond the margins of the etched unit [*Hynek*, 2004] as well as in the process of eroding out from the Meridiani plains (e.g., Figure 5a).

[47] High resolution images from the HiRISE camera extend the morphological similarity of the Arabia Terra deposits with the Meridiani playa deposits down to the submeter scale. Layering in some of the etched terrain deposits exhibits a distinct periodicity (Figure 8a), similar to that seen in Becquerel crater 1200 km to the north (Figure 8b) [*Lewis et al.*, 2008]. This periodic layering is strongly suggestive of climatic control, and is consistent with a climatic modulation of the precipitation and evaporation flux driving variations in the rate groundwater upwelling and evaporation. Layering in other portions of the etched terrain (Figure 8c) superficially resembles that observed in Henry crater (Figure 8d), 1700 km to the southeast. Many of the intracrater deposits exhibit step-like layering, suggestive of strength contrasts within or between layers. This step-like layering is observed both in outliers of the etched terrain (Figures 8e and 8g), and in deposits within Schiapparelli crater 800 km to the east (Figure 8f). Fine-scale layering is also preserved beneath the armoring crater ejecta surrounding pedestal craters (Figure 8h). A periodicity in apparent layer thickness or strength similar to that expressed in Becquerel (Figure 8c) is also observed in the pedestal crater in Figure 8h, and possibly in the deposits in Figures 8c and 8f, though these are not as clearly expressed. That a similar periodicity in the layering is seen in deposits across much of Arabia Terra further strengthens the argument for a commonality of origins.

[48] As a specific comparison of the model predictions with the observed sedimentary record, we focus on two prominent degraded impact basins in eastern Arabia Terra, within which groundwater-mediated sedimentation is predicted (see Figure 4n for context boxes). The models predict deposit thicknesses of approximately 0.5 to 1 km within these basins. MOLA topography reveals the presence of pedestal craters within each of these basins (Figure 9), preserving a remnant of eroded deposits up to 1 km thick that likely covered the basin floors. The apparent periodic bundling of layers within one of these pedestals (Figure 8h) suggests climatic control and a related origin to deposits elsewhere in Meridiani and Arabia Terra. The pedestals are surrounded by smooth and ridged plains units of uncertain origin on the basin floors. The compressional ridges on the basin floors are consistent with the plains being composed of either volcanic or strongly indurated sedimentary materials. While the original extent and thickness of the sedimentary deposits throughout Arabia Terra is uncertain, these and other pedestal craters suggest that much of the region was at one time covered in sedimentary deposits in excess of 1 km in thickness.

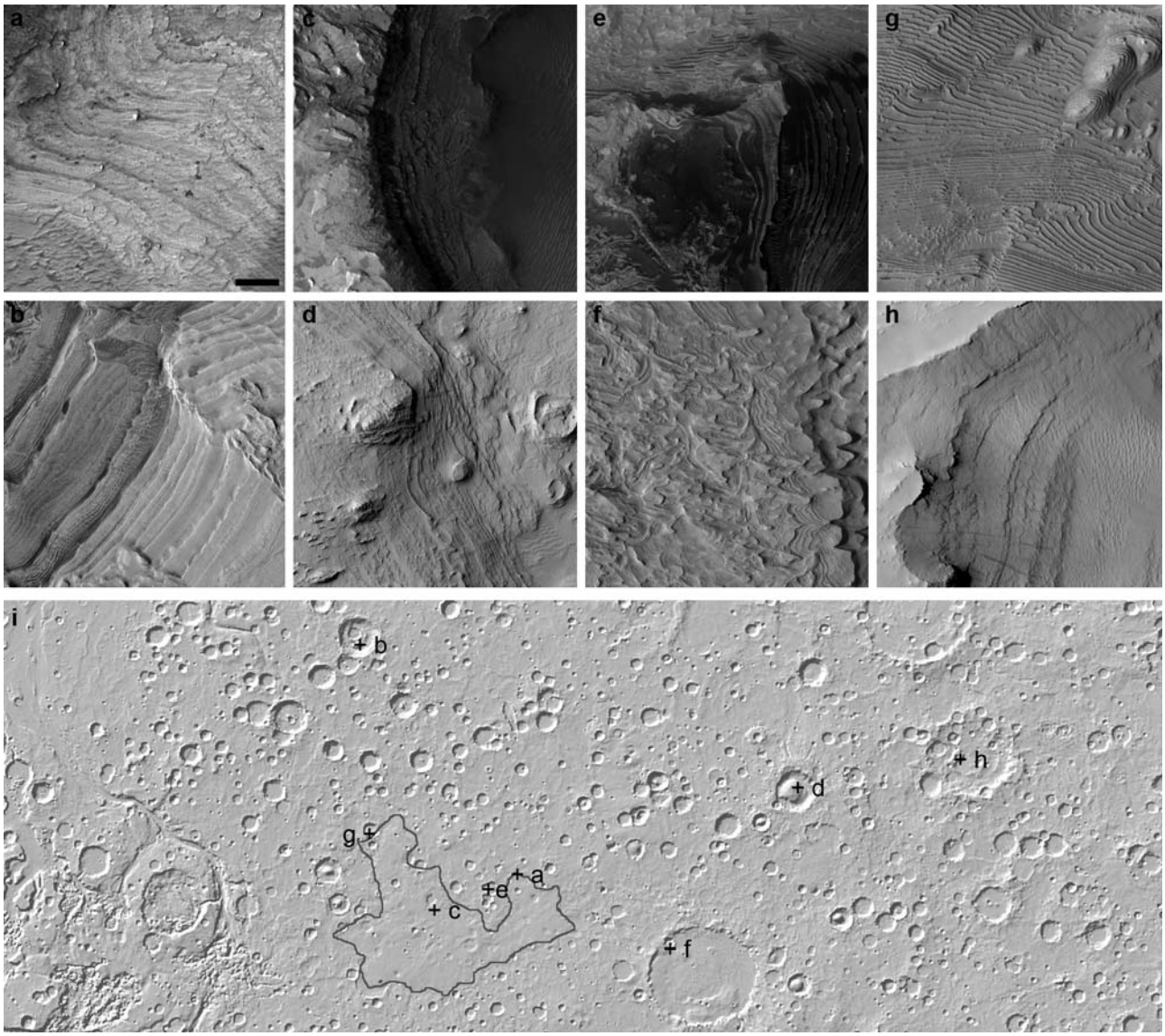

Figure 8. HiRISE images of select representative layered deposits in Arabia Terra. The scale bar in Figure 8a is 25 m in length, and Figures 8a–8h are at the same scale. Deposits within an outlier of the Meridiani etched terrain show evidence for a periodic bundling of layers into packets (Figure 8a, image PSP_007440_1845), similar to periodic variations in layer thickness observed in Becquerel crater by *Lewis et al.* [2008] 1200 km to the northeast (Figure 8b, image PSP_001955_2015). Layering exposed in a crater wall within the Meridiani etched terrain (Figure 8c, image ESP_011910_1825) superficially resembles layering within an intracrater mound in Henry crater 1700 km to the east (Figure 8d, image PSP_009008_1915). Step-like layering observed in outliers of the etched terrain (Figures 8e and 8g, images ESP_012490_1835 and PSP_002878_1880, respectively) resemble step-like layering exposed in deposits within Schiapparelli crater 800 km to the southeast (Figure 8f (right side), PSP_002508_1800). Layering is preserved in a pedestal crater beneath an armoring layer of crater ejecta (Figure 8h, image PSP_7531_1935; see also Figure 10a). A possible periodicity in layer thickness or strength similar to that in Figures 8a and 8b is observed in Figure 8h, though the layering is partially obscured by dust and a thinner stratigraphic section is exposed. This pedestal crater is 1950 km east of the deposits shown in Figure 8a. The locations of images (Figures 8a–8h) are shown in Figure 8i, superimposed over MOLA shaded relief, with the outline of the etched terrain as identified by *Hynek* [2004] outlined for reference.

[49] While aeolian processes likely played a role in both deposition and erosion of the deposits both within and beyond Meridiani [*Fassett and Head*, 2007], this does not satisfactorily explain their concentration in Arabia Terra. The key unknown is not the origin of the clastic grains, since aeolian transport and deposition is ubiquitous on Mars, but rather the cause of their induration and accumulation to thicknesses in excess of a kilometer in this particular region. Our work suggests that hydrological activity leading to evaporite formation and groundwater-mediated cementation

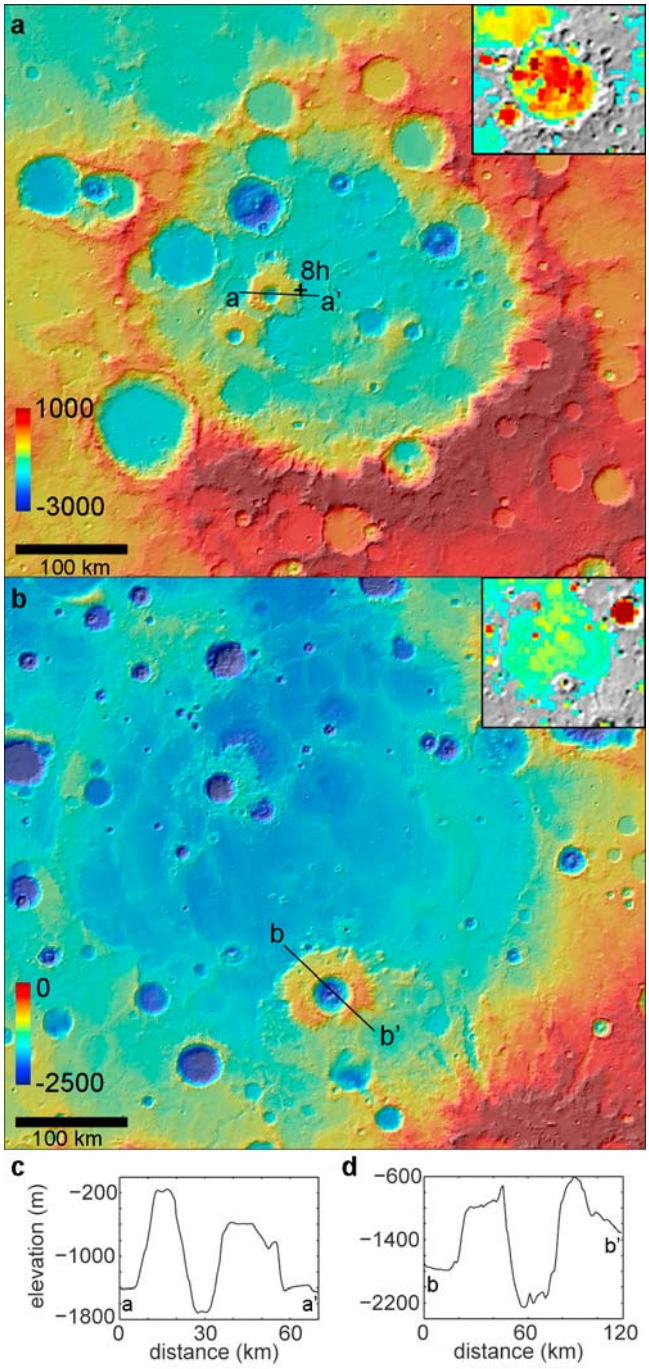

Figure 9. (a–b) Two large degraded impact basins in eastern Arabia Terra, for which the model predicts significant accumulations of evaporites and cemented sediments (insets, see Figure 4n for color scale and context boxes). The basins are floored with smooth to ridged plains materials of uncertain origin. (c–d) Pedestal craters within the basins preserve the remnants of formerly more extensive deposits, suggesting preerosional deposit thicknesses within the basins of up to 1 km. The location of Figure 8h, which reveals periodic bundles of layers, is shown in Figure 9a.

of aeolian debris played a pivotal role in the origin of the Arabia Terra deposits. As aeolian activity continuously redistributed sand and dust across the surface of the planet, these materials would have been infiltrated by groundwater in Arabia Terra. Evaporation of the groundwater at the sediment surface would have precipitated sulfate salts, cementing the materials in place. The resulting gradual aggradation of the surface would have been accompanied by a parallel rise in the water table, allowing accumulation of thick deposits (Figure 10). As the hydrological cycle waned in the early Hesperian, precipitation and evaporation rates would have decreased and the water table would have dropped deeper beneath the surface. The sedimentary deposits across Arabia Terra would then be left above the water table, preventing further induration of the wind-transported sand and dust, and allowing the net deflation of the region to begin. Deposits were preferentially preserved where protected from subsequent erosion by either a lag deposit of hematite concretions or by an armoring layer of crater ejecta.

6. Alternative Interpretations of the Meridiani Planum Deposits

[50] This study focuses on understanding the mechanism required to maintain the groundwater upwelling and playa environment inferred from the rover observations, in contrast with other studies that propose different interpretations of the observations and alternative depositional environments and mechanisms [*Knauth et al.*, 2005; *McCollom and Hynek*, 2005; *Niles and Michalski*, 2009]. Debate continues over the interpretation of the Meridiani deposits, their environment of deposition, and the ultimate source of the sulfates. Within the context of the playa interpretation, we have shown that regional to global scale groundwater flow can explain the location, thickness, dip angle and azimuth, and deposition rate of the deposits, while also making testable predictions regarding the distribution of deposits throughout the Arabia Terra region.

[51] Proposed depositional mechanisms involving volcanic fumaroles [*McCollom and Hynek*, 2005] or impact base surges [*Knauth et al.*, 2005] offer alternative mechanisms for producing the deposit morphology and mineralogy, but do not address the spatial distribution. Impacts are ubiquitous on Mars, and there is no evidence to suggest that impact base surges should take on a different form in Meridiani and Arabia Terra than elsewhere. Furthermore, an impact origin is difficult to reconcile with the observation that the deposits postdate the largest craters in the region and that many craters are filled to their rims with deposits. Similarly, while volcanic processes have been widespread on Mars over its history, the observed deposits do not have any clear relationship to known volcanic vents. For both impact and volcanic interpretations, some special circumstance must be invoked in order to explain the localization of the deposits to Arabia Terra. Furthermore, these mechanisms do not adequately explain the association of similar sulfate and hematite deposits with regions of unambiguous groundwater outflow in the chaos regions and Valles Marineris canyons [*Gendrin et al.*, 2005; *Glotch and Christensen*, 2005; *Glotch and Rogers*, 2007; *Noe Dobrea et al.*, 2008;

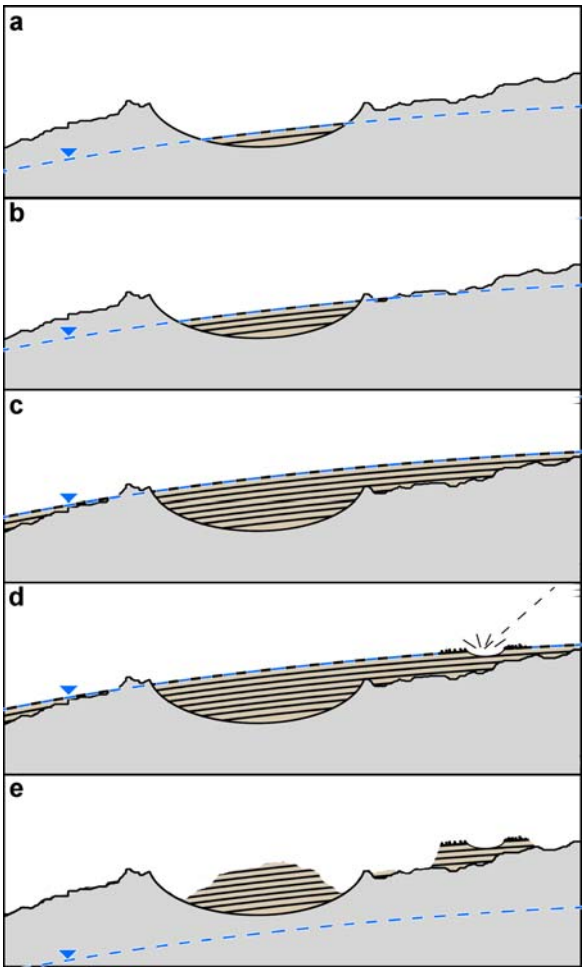

Figure 10. Cartoon diagram of sequence of events in the evolution of the Arabia Terra deposits. The water table is denoted by the blue line and marked with an inverted triangle. Ancient crust is shown in gray, and sedimentary deposits shown in beige with layering in black. (a) Early groundwater evaporation is limited to the largest impact craters. (b–c) As the craters fill with sediments, the water table rises until the groundwater-driven playa expands laterally over the intercrater plains. (d) Portions of the deposit become armored by ejecta from impacts or by the accumulation of a lag of hematite concretions as in Meridiani, or may simply be more resistant to erosion due to a greater degree of induration. (e) A subsequent drop in the water table exposes the deposits to aeolian deflation, leaving behind thick intracrater deposits and isolated remnants of deposits in the form of pedestal craters or other plains-covering deposits.

Weitz et al., 2008; *Lichtenberg et al.*, 2010], which argue strongly for a groundwater origin for the Meridiani deposits.

[52] Several arguments against the playa hypothesis for the origin of the deposits have been framed around the elemental abundance data from the rover observations. *McCollom and Hynek* [2005] argued that the elemental abundances observed in the Meridiani outcrops were best matched by the addition of pure SO_2 to unweathered basalt, though *Squyres et al.* [2006] demonstrated that the data was best fit by a mixture of weathered basalt and (Mg, Fe, Ca) SO_4 as predicted by the playa hypothesis. *Niles and Michalski* [2009] argued that closed system weathering provides the best explanation for the elemental abundances. They note that the scatter in elemental abundance data is reasonably fit by simply adding or subtracting $MgSO_4$. The fact that the majority of the chemical variation within the Meridiani outcrops is best explained by $MgSO_4$ mobility is expected, since epsomite ($MgSO_4 \cdot 7\ H_2O$) is the last and most soluble mineral precipitated during evaporation of basaltic weathering fluids in thermodynamic modeling [*Tosca et al.*, 2005]. The composition of the deposits would have been largely homogenized by mixing of grains during aeolian transport and redeposition within the paleo dune field. Later episodes of groundwater-mediated diagenesis would preferentially dissolve $MgSO_4$ from the sediments lower in the sequence, resulting in the observed decrease in Mg and S with depth [*Squyres et al.*, 2009].

[53] The key question is the nature and origin of the material prior to this late diagenesis. *Niles and Michalski* [2009] note that the relative cation abundances aside from Mg are close to those in unaltered basalt, which they interpret as evidence for closed system alteration within an ice cap. A relatively homogenous composition is consistent with the broad regions of nearly uniform groundwater upwelling predicted by the hydrological models (Figure 4o). The Opportunity rover has sampled only a small fraction of the full horizontal and vertical extent of the Meridiani deposit of approximately 1000 km and 1 km, respectively. Closed system alteration of basaltic grains would require that the entire Meridiani deposit have basaltic cation abundances. While observations are limited by the range of the Opportunity rover and the vertical exposure of the outcrops, elemental abundance data from Victoria Crater reveals Fe enrichments relative to other elements of approximately 20% in comparison with the outcrops at Endurance Crater [*Squyres et al.*, 2009]. Orbital observations reveal lateral mineralogical heterogeneity within Meridiani, with variations in the hydration state of sulfates, strength of the sulfate signature in the spectra, and degree of induration [*Wiseman et al.*, 2010]. These orbital observations are consistent with, but do not require, significant heterogeneity in the elemental composition of the deposits as well.

[54] Perhaps the strongest argument for an open system origin for the deposits involving groundwater is the identification of spectrally and geomorphically similar sulfate-hematite deposits at the sources of the outflow channels in chaos regions and the Valles Marineris canyons [*Gendrin et al.*, 2005; *Glotch and Christensen*, 2005; *Glotch and Rogers*, 2007; *Noe Dobrea et al.*, 2008; *Weitz et al.*, 2008; *Lichtenberg et al.*, 2010]. A closed system source for these deposits is at odds with the unambiguous geomorphic evidence for the release of enormous quantities of groundwater from these regions. The vast amounts of groundwater required to carve the outflow channels requires that the chaos regions tap aquifers of substantial regional extent [*Andrews-Hanna and Phillips*, 2007].

[55] It has also been argued that deeply sourced fluids in a basaltic aquifer are inconsistent with the inferred acidity of the fluids at the surface [*Niles and Michalski*, 2009]. While the fluids may indeed be buffered at a near-neutral pH in the deep subsurface, as the slowly upwelling groundwater nears the oxidized surface environment, oxidation of the groundwater would be accompanied by increasing acidity [*Burns*,

1993; *Burns and Fisher*, 1993; *Hurowitz et al*., 2010]. Within the playa, the rise and fall of the water table and contemporaneous aeolian reworking of the sediments would be highly effective in oxidizing both the sediments and fluids near the surface. Evaporitic concentration of the basaltic weathering fluids would continue to lower the pH [*Tosca et al.*, 2005]. Furthermore, the presence of Fe/Mg smectites lower in the stratigraphic column argues for formation of some portions of the deposit under higher pH conditions [*Wiseman et al.*, 2010].

[56] Previous studies have raised arguments against the playa hypothesis on the basis of the large horizontal extent of the deposits, the large volumes of groundwater required, and the lack of an enclosed basin [*McCollom and Hynek*, 2005; *Niles and Michalski*, 2009]. This work addresses each of these objections. We have shown that regional-scale groundwater flow patterns would have maintained a playa environment not only in Meridiani Planum, but also across much of Arabia Terra. Growth of the deposits smoothes the surface topography, allowing horizontally continuous deposits over distances of many 100s of km, with consistent dip directions approximately following the regional slopes, as found by *Hynek and Phillips* [2008]. The regional nature of the groundwater flow would also allow for consistent composition of the deposits across great distances. The groundwater upwelling in the absence of an enclosed basin is driven by the unique topography of Arabia Terra relative to the highlands and lowlands. The predicted rates of groundwater upwelling could generate the observed deposit thickness in timescales of 10s to 100s of Myr, depending on the assumed fluid salinity and aquifer properties.

[57] It has been suggested that the groundwater discharge at Meridiani Planum may have resulted from Tharsis-induced tilting of the crust and lithosphere in Arabia Terra [*Hynek and Phillips*, 2005; *Arvidson et al.*, 2006b]. However, in previous work we investigated the hydrological evolution of Mars before, during, and after Tharsis formation, and found Meridiani Planum to emerge as a region of focused groundwater upwelling in all three cases [*Andrews-Hanna et al.*, 2007]. The groundwater upwelling is driven rather by a combination of a precipitation-evaporation-driven hydrological cycle and the regional topography of Arabia Terra. The slopes in Arabia Terra are primarily a result of isostatically compensated crustal thickness variations [e.g., *Neumann et al.*, 2004]. Our loading models suggest that the modeled Tharsis-induced changes in slope outside the rise are one to two orders of magnitude less than the preexisting slopes associated with the isostatic crustal thickness variations of the dichotomy and Arabia Terra [*Andrews-Hanna et al.*, 2007]. Localized admittance values in Arabia Terra require a thin lithosphere at the time of formation [*Evans et al.*, 2010], suggesting that the low topography of this region was established early in Mars history. This is consistent with the interpretation of Arabia Terra as a partial ring structure around the Borealis impact basin [*Andrews-Hanna et al.*, 2008]. While Tharsis undoubtedly did affect the hydrological evolution of Mars, it did not play a dominant role in maintaining the Meridiani playa.

[58] It has been suggested that groundwater flow on Mars was only regional in extent, based on the lack of outflow features in regions of predicted groundwater outflow in western Hellas and other regions at the time of formation of the Hesperian outflow channels [*Harrison and Grimm*, 2009]. While the assumption of a globally interconnected aquifer system is not appropriate for the Earth, such large-scale interconnection on Mars is suggested by the uniform impact bombardment of the southern highlands, which would have intensely fractured the crust over the entire surface of Noachian Mars [*Clifford*, 1981, 1993]. We see no evidence for impermeable aquicludes subdividing aquifers within the southern highlands. The lack of evidence for outflows within Hellas may have been a result of a possible ice-covered sea within the basin at the time [*Moore and Wilhelms*, 2001], or may suggest the importance of more local pressurization mechanisms at the sources of the outflow channels during the Hesperian. However, a source for the Meridiani fluids from regional groundwater flow does not require a globally interconnected aquifer, rather only that aquifers be interconnected from the hydraulic divide between Arabia Terra and Hellas through to the proximal portions of the northern lowlands. Indeed the strong agreement between predicted and observed loci of groundwater upwelling in Arabia Terra provides compelling evidence in favor of long distance groundwater flow and aquifers that were interconnected on at least regional scales on early Mars.

7. Discussion

[59] These results show that late Noachian-early Hesperian evaporitic sulfate deposits in Meridiani Planum were a natural result of groundwater upwelling in a precipitation-evaporation-driven hydrological cycle operating under arid conditions. Meridiani and the surrounding Arabia Terra region are among the few regions of presently exposed Noachian-aged crust for which sustained groundwater upwelling and evaporation is predicted. A steady flux of groundwater to the surface would have sustained regional playa development in the absence of a topographic basin, driven by the combination of the general low topography of Arabia Terra and the distinct breaks in slope separating it from the southern highlands and northern lowlands. Groundwater evaporation would have produced deposits of substantial thickness, both through the direct precipitation of evaporites and the cementation and induration of aeolian sediments. Results suggest a temporal evolution, in which groundwater upwelling is first restricted to isolated depressions and craters, but then spreads laterally across the surface as these depressions fill with deposits.

[60] Deposits similar to the Meridiani sediments are predicted to be widespread across much of Arabia Terra. Multiple lines of evidence suggest that Arabia Terra was a nexus of hydrological activity throughout the Noachian and early Hesperian epochs. Observations of sediment-filled craters, inverted valley networks, widespread layered mantling deposits, pedestal craters, and the Meridiani playa evaporites are all consistent with the model prediction of sustained groundwater upwelling and evaporation in Arabia Terra. Variations in the morphology and composition of the deposits likely result from varying proportions of evaporitic and clastic materials, possibly driven by variations in either the groundwater flux or sediment supply. The hydrological

models successfully explain the spatial distribution, rate of deposition, thickness, and dip of the Arabia Terra deposits.

[61] This long-wavelength groundwater flow is similar to that found in arid regions of the Earth, such as the Great Artesian Basin of Australia [*Habermehl*, 1980]. This hydrological cycle requires active precipitation-induced recharge of the low latitude aquifers, though this precipitation could have been in the form of either rain or snow, provided that the snow was able to melt and infiltrate the surface. The regional to global nature of the hydrological cycle is not consistent with spatially and temporally isolated impact-induced greenhouse climates [*Segura et al.*, 2002], or localized volcanic warming of the subsurface [*McCollom and Hynek*, 2005]. While local hydrothermal circulation can elevate the hydraulic head over small regions, the hydrological cycle responsible for Meridiani evaporite formation requires long distance cycling of water between the lowlands and highlands, and is incompatible with the typical length scales of hydrothermal groundwater circulation [*Travis et al.*, 2003]. At the locations of groundwater upwelling, the formation of playa evaporites requires temperatures above the freezing point of the groundwater brines. Conditions conducive to both precipitation-induced aquifer recharge and groundwater evaporation must have been stable or episodically present over long periods of time (likely 10s to 100s of Myr) over much of the surface of Mars in order to establish and maintain the hydrological cycle. A groundwater-driven playa origin for the Meridiani deposits thus implies that conditions conducive to life persisted across much of the low latitudes to midlatitudes of Mars as late as the early Hesperian.

[62] The detailed in situ observations by the Mars Exploration Rover Opportunity reveal the specific local depositional environment and modification history of the Meridiani deposits: that they are composed of dirty evaporites that have been substantially reworked by aeolian and fluvial processes and diagenetically modified by a fluctuating water table, consistent with formation in a playa. The hydrological modeling results presented here reveal the deeper mechanisms at work and the broader hydrologic and climatic implications of the deposits: that they formed as a result of sustained regional groundwater upwelling in response to a precipitation-evaporation-driven hydrological cycle operating in an arid climate, with the location of the deposits resulting from the unique topography of the surrounding Arabia Terra region. This work highlights the importance of combining in situ and orbital observations with a theoretical understanding of the hydrological cycle.

Appendix A: Model Details

[63] The hydrological model represents unconfined groundwater flow using the Dupuit approximation [*Demming*, 2002], which assumes that the hydraulic gradients are sufficiently small that flow lines are horizontal and vertical flow can be neglected. These assumptions are reasonable approximations for the long-wavelength groundwater flow of interest here. Equation 1 was discretized over a uniform latitude-longitude grid. Additional "cap cells" were added at the poles in hydrologic communication with all cells in the adjacent row, allowing continuous flow and a smooth variation in hydraulic head across the poles.

[64] The aquifer porosity and hydraulic conductivity were taken from the megaregolith model of *Hanna and Phillips* [2005]. The depth dependence of the aquifer properties in this model is generally similar to other models [*Clifford*, 1993; *Clifford and Parker*, 2001; *Wang et al.*, 2006], and our investigation of a range of parameter space shows that the results of this study are not strongly sensitive to the specific aquifer model. The discontinuity in the porosity at the base of the megaregolith at 2 km depth in the aquifer model of *Hanna and Phillips* [2005] is smoothed to a cosine transition between 1 and 3 km in order to improve the model stability. The aquifer properties are updated to reflect the changing hydraulic head once every 10 time steps, which decreases the model run time without adversely affecting performance.

[65] Global models were typically run at a spatial resolution of 2.5 degrees per pixel, a limitation imposed by the model run times. These models are at a higher resolution than the 5 degrees per pixel results presented earlier [*Andrews-Hanna et al.*, 2007]. Higher resolution simulations were performed globally at 1.25 degrees per pixel, and locally at 0.25 degrees per pixel over a limited region, as discussed in the main text.

Appendix B: Model Benchmarking

[66] The full model representing two-dimensional unconfined groundwater flow in a spherical shell with depth-dependent hydraulic conductivity and porosity is not amenable to analytic solutions. Benchmarking was performed with a simplified model in an aquifer with uniform porosity and hydraulic conductivity. In the limit of high model resolution over regions of limited size, the effect of the planetary curvature on the flow will be unimportant and the model results should be reasonably approximated by analytic solutions in one- or two-dimensional Cartesian geometries. We applied constant head boundary conditions at two ends of a one-dimensional strip of constant elevation within the model, subject to lateral no-flow boundary conditions and a constant rate of recharge at the surface. For unconfined flow under Dupuit assumptions, the hydraulic head should follow a parabolic profile, and the model results agreed with the analytic solutions to the percent level. The model was also benchmarked against two-dimensional analytic solutions for unconfined aquifer drawdown surrounding a well in which a constant pumping rate is applied [*Demming*, 2002], with the errors again less than the percent level. The model was benchmarked against simpler 1-D radially symmetric numerical models, showing perfect agreement. As a test of the spherical geometry of the model, the diffusion of a hemispheric step function in hydraulic head was repeated with the step function oriented either north-south or east-west, demonstrating that the longitudinal flow across the model edges and latitudinal flow across the poles are accurately represented in the models.

[67] While the full model cannot be benchmarked against an analytic solution, it can be tested for conservation of water volume. In equilibrium, continued flow driven by the precipitation and evaporation boundary conditions should

maintain a constant volume of water in the aquifers. The total water inventory was tracked during model simulations, and a small numerical drift was found to result, likely from a combination of the discretization of the equations of flow and numerical rounding errors. This drift was found to be first order in time and second order in space, as would be expected for the fully explicit finite difference formulation. For short-term simulations (e.g., the one-time diffusion of a hydraulic step function), this numerical drift was inconsequential to the results. However, in the long term simulations with sustained evaporation and recharge, the numerical drift would accumulate to nontrivial levels on timescales of ~100 Myr, effectively changing the total water inventory over time. In order to allow for long-term simulations, the total fluid volume within the aquifers was tracked during the simulations and a correction term was added to the precipitation in order to maintain conservation of fluid volume. This drift correction generally modified the precipitation rate by less than 1%. Increasing the spatial or temporal resolution decreased the drift correction, but also resulted in increased model run times. Since this correction term is much less than expected natural spatial and temporal variations in the distribution and rate of precipitation, we expect it has a negligible effect on the results and conclusions.

Appendix C: Parameter Sensitivity

[68] Martian hydrological models are inherently under constrained. We have no direct data relevant to the hydrological properties of the subsurface, or how those properties vary in space and time. We employ the hydrological model of *Hanna and Phillips* [2005], which estimates likely ranges of the porosity, permeability, and compressibility using a combination of terrestrial measurements, and terrestrial and lunar analog materials. In that model, the permeability ranges from 10^{-15} to 10^{-11} m^2, the porosity ranges from 0.16 to 0.04, and the compressibility ranges from 2×10^{-9} to 1.5×10^{-10} Pa^{-1} between the surface and a depth of 10 km. These values are broadly similar to those in other hydrological models of Mars [*Clifford*, 1993; *Clifford and Parker*, 2001; *Wang et al.*, 2006] and the Earth [*Manning and Ingebritsen*, 1999; *Saar and Manga*, 2004]. Of these parameters, the greatest uncertainty lies in the permeability, which varies by several orders of magnitude within terrestrial aquifers. The permeability determines the equilibrium hydrological state of the planet, while the aquifer porosity and compressibility (for the case of confined aquifers) affect only the time-dependent hydrological response.

[69] The patterns of groundwater flow and distribution of groundwater upwelling is insensitive to a uniform scaling of any of the relevant aquifer properties. For example, if the permeability is increased globally by a constant factor, this scaling factor will come out in front of the derivatives in the first term in equation (1) and the precipitation rate increases by a similar factor, resulting only in a scaling of the rate of temporal evolution of the system. This was confirmed in a model with a tenfold increase in permeability, with the results after 5 Myr of evaporite deposition being identical within the numerical precision to those in the nominal model after 50 Myr.

[70] We also consider a model in which the vertical permeability structure within the aquifer is changed, with the ratio of the permeability at the surface to that at a depth of 10 km decreased by a factor of 10. This is implemented in terms of the hydrological model of *Hanna and Phillips* [2005] by decreasing the maximum aperture of fractures at the surface while holding the minimum aperture at depth constant. This change in the vertical permeability structure has a noticeable effect on the global distribution of groundwater and surface evaporation. In particular, a greater drawdown of the water table is observed around the Hellas impact basin than observed in the baseline model. The more rapid decrease in permeability with depth in the baseline model impedes the aquifer drawdown around Hellas. As the water table drops deeper beneath the surface, the mean aquifer permeability decreases, thereby impeding flow toward the basin and increasing the concavity of the drawdown cone. However, the predicted distribution of sedimentary deposits in Arabia Terra remains largely the same in both models.

[71] Model results would also likely be affected by horizontal anisotropy in the aquifer permeability. Orbital observations reveal evidence for water-mediated bleaching around deformation bands in Arabia Terra and elsewhere [*Okubo and McEwen*, 2007; *Okubo et al.*, 2007]. Compressional deformation bands may act as barriers to the flow, while tensile or shear deformation bands may act as conduits to the flow, with both tending to channel groundwater parallel to the structures. The horizontal stress directions in the Martian lithosphere are dominated by Tharsis loading, with the greatest (compressional) principle stress direction generally oriented radial to Tharsis outside of the rise, leading to circumferential wrinkle ridges. Resulting tectonism and deformation of the crust would act to deflect groundwater flow in a north-south direction in Arabia Terra. As a result, groundwater may follow paths oblique to the regional hydraulic gradients. However, because of the large horizontal extent of Arabia Terra and the consistency of slopes across this region, we expect the general conclusions of this study to be unchanged for the case of aquifer anisotropy.

[72] Lateral variability in the aquifer properties may have also influenced the groundwater flow patterns and resulting deposits. Adopting an approach similar to that of *Harrison and Grimm* [2009], we have investigated the effect of spatially varying aquifer properties. As in that study, the aquifer hydraulic conductivity in each model cell was scaled by a spatially varying factor from the nominal value for that cell. Following *Harrison and Grimm* [2009], we construct this scaling function as a randomly varying logarithmic factor with a variance of 0.5 and a correlation length of 15° on the surface (Figure C1a). A total of 30 realizations of this spatially varying random scaling function were generated, and the hydraulic evolution simulated for each. The model run times were accelerated by a factor of 5 by artificially increasing the ratio of the deposition rate to the evaporation rate, which was found to have a minimal effect on the resulting evaporite distribution. The hydraulic conductivity scaling factor and resulting deposit distribution from a single randomly selected model are shown in Figures C1a and C1b. The mean (±one standard deviation) deposit thickness agrees well with that predicted by the uniform aquifer model (Figures C1c–C1e). The mean deposits are more broadly

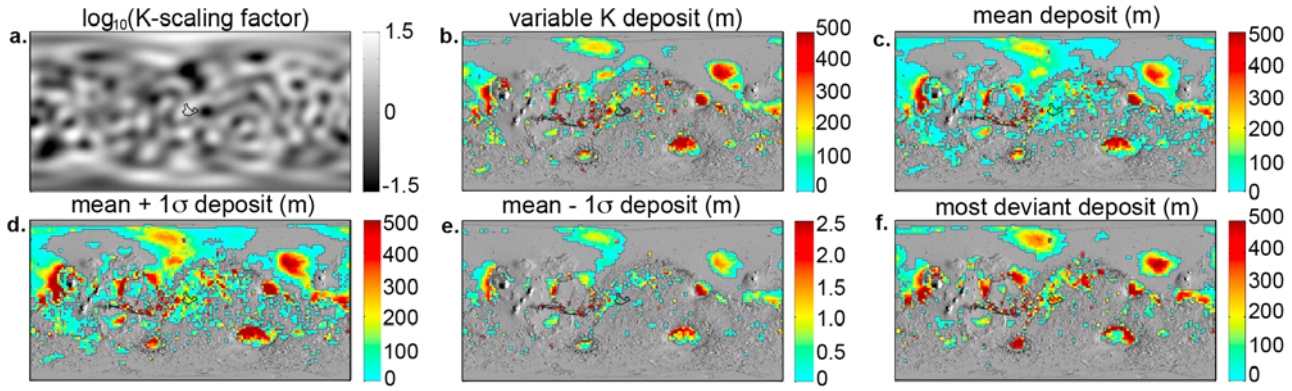

Figure C1. Effect of spatially varying aquifer hydraulic conductivity. (a) The $\log_{10}$ of the hydraulic conductivity scaling factor for a single realization of the laterally heterogeneous aquifer model. (b) The predicted deposit thickness from this single model and (c–e) the mean and ± 1 standard deviation deposit thickness for the full suite of 30 models are consistent with the predictions for the globally uniform model (Figure 2k). (f) The model outcome that deviates most strongly from the mean distribution.

distributed across the surface due to the variations in loci of groundwater upwelling from one model to another. The results of the single model outcome that differs most from the mean distribution of deposits is presented in Figure C1f. Interestingly, this most deviant model results in a thicker deposit more localized to the Meridiani etched terrain than predicted by the uniform aquifer model. All models clearly predict significant evaporite deposition in Meridiani Planum and the Arabia Terra region. Modest variations from one model to another provide both better and worse matches to the observed deposit distribution. In general we find that lateral heterogeneity in the aquifer properties results in only modest changes to the predicted distribution of deposits. Given the lack of constraints on the actual spatial vari-

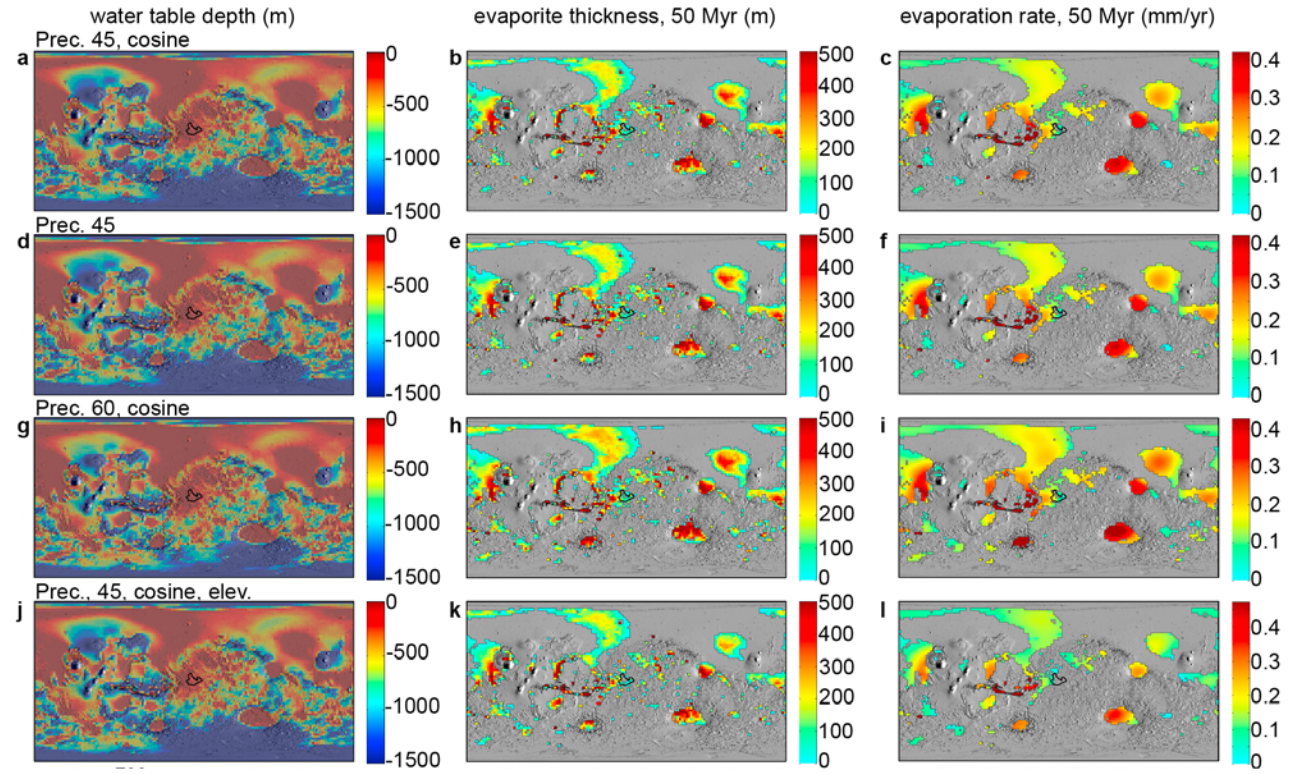

Figure C2. (a–c) Predicted depth to the water table, evaporite thickness, and evaporation rate for different assumed precipitation distributions, including a cosine distribution between ± 45° latitude, (d–f) a uniform distribution between ± 45° latitude, (g–i) a cosine distribution between ± 60° latitude, (j–l) and a cosine distribution between ± 45° latitude scaled by a factor proportional to the local elevation. Similar distributions of evaporite deposits are predicted in all cases.

ability, the results of the uniform aquifer model are most representative of the likely distribution of deposits.

[73] The assumed distribution of precipitation on the surface can also affect the hydrological evolution. The nominal model distributed the precipitation in a longitudinally uniform belt following a half cosine distribution with latitude between ± 45°. We have performed simulations with a uniform distribution between ± 45°, as well as a half cosine distribution between ± 60° latitude. Finally, we considered a model in which the precipitation rate depends on both latitude and elevation, with the half cosine precipitation distribution between ± 45° latitude scaled by a factor varying linearly between elevations of 2 and 5 km. Some elevation dependence of the precipitation rate is suggested by the observation that valley network densities are greater at higher elevations [*Carr*, 1995]. However, this relationship is likely biased by the apparent lack of valley networks in the low elevation Arabia Terra region. Subsequent studies found evidence for inverted channels in this region representing a population of buried and exhumed valley networks [*Williams*, 2007]. In all models, we observe some variability in the predicted depth to the water table, but the global patterns remain the same (Figure C2). Only minor changes in the predicted distribution of deposits are observed, with all models predicting significant evaporite deposits in Arabia Terra.

[74] Models with resolutions ranging from 2.5 degrees per pixel to 0.25 degrees per pixel predict similar distributions of groundwater, but different precipitation rates as discussed in the text. Differences in the regional water table heights of a few hundred meters are observed prior to any evaporite deposition, driven by the effects of smaller craters in the high resolution models as discussed above. As evaporite deposition smoothes the short wavelength topography in regions of active evaporite deposition, the higher resolution model results converge with the lower resolution models.

[75] This parameter investigation demonstrates that the general conclusions of this study are robust despite large uncertainties in the aquifer properties and the ancient precipitation distribution. The one parameter that does exert a dominant control on the hydrological evolution of Mars is the total water inventory (expressed in terms of the initial mean water table depth in the models). However, rather than being a simple source of uncertainty, this a parameter likely experienced real secular and periodic variations with time due to climatic forcing, as discussed in the companion paper (manuscript in preparation, 2010).

[76] **Acknowledgments.** This work was supported by a grant to J.C. A-H by the NASA Mars Data Analysis Program. We are grateful to Joyce Hoopes for assistance in compiling the HiRISE images used in this paper. This manuscript benefited from thorough and thoughtful reviews by Tim Glotch and an anonymous reviewer.

References

Andrews-Hanna, J. C., and R. J. Phillips (2007), Hydrological modeling of outflow channels and chaos regions, *J. Geophys. Res.*, *112*, E08001, doi:10.1029/2006JE002881.

Andrews-Hanna, J. C., R. J. Phillips, and M. T. Zuber (2007), Meridiani Planum and the global hydrology of Mars, *Nature*, *446*, 163–166, doi:10.1038/nature05594.

Andrews-Hanna, J. C., M. T. Zuber, and W. B. Banerdt (2008), The Borealis Basin and the origin of the Martian crustal dichotomy, *Nature*, *453*, 1212–1215, doi:10.1038/nature07011.

Arvidson, R. E., et al. (2006a), Nature and origin of the hematite-bearing plains of Terra Meridiani based on analyses of orbital and Mars Exploration Rover data sets, *J. Geophys. Res.*, *111*, E12S08, doi:10.1029/2006JE002728.

Arvidson, R. E., S. W. Squyres, B. C. Clark, J. P. Grotzinger, A. H. Knoll, S. M. McLennan, and N. J. Tosca (2006b), Regional setting and model for the Meridiani planum deposits investigated by the Opportunity Mars Exploration Rover, *Lunar Planet. Sci.*, *XXXVII*, Abstract 1400.

Barnhart, C. J., A. D. Howard, and J. M. Moore (2009), Long-term precipitation and late-stage valley network formation: Landform simulations of the Parana Basin, Mars, *J. Geophys. Res.*, *114*, E01003, doi:10.1029/2008JE003122.

Bibring, J.-P., et al. (2006), Global mineralogical and aqueous Mars history derived from OMEGA/Mars Express data, *Science*, *312*, 400–404, doi:10.1126/science.1122659.

Boynton, W. V., et al. (2002), Distribution of hydrogen in the near surface of Mars: Evidence for subsurface ice deposits, *Science*, *297*, 81–85, doi:10.1126/science.1073722.

Brain, D. A., and B. M. Jakosky (1998), Atmospheric loss since the onset of the Martian geologic record: Combined role of impact erosion and sputtering, *J. Geophys. Res.*, *103*, 22,689–22,694, doi:10.1029/98JE02074.

Burns, R. G. (1993), Rates and mechanisms of chemical weathering of ferromagnesium silicate minerals on Mars, *Geochim. Cosmochim. Acta*, *57*, 4555–4574, doi:10.1016/0016-7037(93)90182-V.

Burns, R. G., and D. S. Fisher (1993), Rates of oxidative weathering on the surface of Mars, *J. Geophys. Res.*, *98*, 3365–3372, doi:10.1029/92JE02055.

Carr, M. H. (1995), The Martian drainage system and the origin of valley networks and fretted channels, *J. Geophys. Res.*, *100*, 7479–7507, doi:10.1029/95JE00260.

Carr, M. H., and F. C. Chuang (1997), Martian drainage densities, *J. Geophys. Res.*, *102*, 9145–9152, doi:10.1029/97JE00113.

Carr, M. H., and J. W. Head (2003), Basal melting of snow on early Mars: A possible origin of some valley networks, *Geophys. Res. Lett.*, *30*(24), 2245, doi:10.1029/2003GL018575.

Carr, M. H., and M. C. Malin (2000), Meter-scale characteristics of Martian channels and valleys, *Icarus*, *146*, 366–386, doi:10.1006/icar.2000.6428.

Christensen, P. R., et al. (2000), Detection of crystalline hematite mineralization on Mars by the Thermal Emission Spectrometer: Evidence for near surface water, *J. Geophys. Res.*, *105*, 9623–9642, doi:10.1029/1999JE001093.

Christensen, P. R., R. V. Morris, M. D. Lane, J. L. Bandfield, and M. C. Malin (2001), Global mapping of Martian hematite mineral deposits: Remnants of water-driven processes on early Mars, *J. Geophys. Res.*, *106*, 23,873–23,885, doi:10.1029/2000JE001415.

Clifford, S. M. (1981), A pore volume estimate of the Martian megaregolith based on a lunar analog, *LPI Contrib.*, *441*, 46–48.

Clifford, S. M. (1993), A model for the hydrologic and climatic behavior of water on Mars, *J. Geophys. Res.*, *98*, 10,973–11,016, doi:10.1029/93JE00225.

Clifford, S. M., and T. J. Parker (2001), The evolution of the Martian hydrosphere: Implications for the fate of a primordial ocean and the current state of the northern plains, *Icarus*, *154*, 40–79, doi:10.1006/icar.2001.6671.

Cloutis, E. A., et al. (2006), Detection and discrimination of sulfate minerals using reflectance spectroscopy, *Icarus*, *184*, 121–157, doi:10.1016/j.icarus.2006.04.003.

Craddock, R. A., and A. D. Howard (2002), The case for rainfall on a warm, wet early Mars, *J. Geophys. Res.*, *107*(E11), 5111, doi:10.1029/2001JE001505.

Demming, D. (2002), *Introduction to Hydrology*, 468 pp., McGraw Hill, New York.

Edgett, K. S., and M. Malin (2002), Martian sedimentary rock stratigraphy: Outcrops and interbedded craters of northwest Sinus Merdiani and southwest Arabia Terra, *Geophys. Res. Lett.*, *29*(24), 2179, doi:10.1029/2002GL016515.

Evans, A. J., J. C. Andrews-Hanna, and M. T. Zuber (2010), Geophysical limitations on the erosion history within Arabia Terra, *J. Geophys. Res.*, doi:10.1029/2009JE003469, in press.

Fassett, C. I., and J. W. Head (2007), Layered mantling deposits in northeast Arabia Terra, Mars: Noachian-Hesperian sedimentation, erosion, and terrain inversion, *J. Geophys. Res.*, *112*, E08002, doi:10.1029/2006JE002875.

Fassett, C. I., and J. W. Head (2008), Valley network-fed, open-basin lakes on Mars: Distribution and implications for Noachian surface and subsurface hydrology, *Icarus*, *198*, 37–56, doi:10.1016/j.icarus.2008.06.016.

Feldman, W. C., et al. (2004), Global distribution of near-surface hydrogen on Mars, *J. Geophys. Res.*, *109*, E09006, doi:10.1029/2003JE002160.

Gendrin, A., et al. (2005), Sulfates in Martian layered terrains: The OMEGA/Mars Express view, *Science*, *307*, 1587–1591, doi:10.1126/science.1109087.

Glotch, T. D., and J. L. Bandfield (2006), Determination and interpretation of surface and atmospheric Miniature Thermal Emission Spectrometer spectral end-members at the Meridiani Planum landing site, *J. Geophys. Res.*, *111*, E12S06, doi:10.1029/2005JE002671.

Glotch, T. D., and P. R. Christensen (2005), Geologic and mineralogic mapping of Aram haos: Evidence for a water-rich history, *J. Geophys. Res.*, *110*, E09006, doi:10.1029/2004JE002389.

Glotch, T. D., and A. D. Rogers (2007), Evidence for aqueous deposition of hematite- and sufate-rich light-toned layered deposits in Aureum and Iani chaos, Mars, *J. Geophys. Res.*, *112*, E06001, doi:10.1029/2006JE002863.

Golombek, M. P., J. A. Grant, L. S. Crumpler, R. E. Arvidson, J. F. Bell, C. M. Weitz, R. J. Sullivan, P. R. Christensen, L. A. Soderblom, and S. W. Squyres (2006), Erosion rates at the Mars Exploration Rover landing sites and long-term climate change on Mars, *J. Geophys. Res.*, *111*, E12S10, doi:10.1029/2006JE002754.

Grant, J. A., and P. H. Schultz (1990), Gradational epochs on Mars: Evidence from west-northwest of Isidis basin and Electris, Icarus, 84, 166–195, doi:10.1016/0019-1035(90)90164-5.

Greeley, R., and J. E. Guest (1987), Geologic map of the eastern equatorial region of Mars, *U.S. Geol. Surv. Misc. Invest. Map*, I-1802-B.

Griffes, J. L., R. E. Arvidson, F. Poulet, and A. Gendrin (2007), Geologic and spectral mapping of etched terrain deposits in northern Meridiani Planum, *J. Geophys. Res.*, *112*, E08S09, doi:10.1029/2006JE002811.

Grotzinger, J. P., et al. (2005), Stratigraphy and sedimentology of a dry to wet eolian depositional system, Burns formation, Meridiani Planum, Mars, *Earth Planet. Sci. Lett.*, *240*, 11–72, doi:10.1016/j.epsl.2005.09.039.

Habermehl, M. A. (1980), The Great Artesian Basin, Australia, *J. Aust. Geol. Geophys.*, *5*, 9–38.

Handford, C. R. (1991), Marginal marine halite: Sabkhas and salinas, in *Evaporites, Petroleum, and Mineral Resources*, edited by J. L. Melvin, pp. 1–66, Elsevier, New York.

Hanna, J. C., and R. J. Phillips (2005), Hydrological modeling of the Martian crust with application to the pressurization of aquifers, *J. Geophys. Res.*, *110*, E01004, doi:10.1029/2004JE002330.

Harrison, K. P., and R. E. Grimm (2008), Multiple flooding events in the Martian outflow channels, *J. Geophys. Res.*, *113*, E02002, doi:10.1029/2007JE002951.

Harrison, K. P., and R. E. Grimm (2009), Regionally compartmented groundwater flow on Mars, *J. Geophys. Res.*, *114*, E04004, doi:10.1029/2008JE003300.

Houston, J. (2006), Variability of precipitation in the Atacam Desert: Causes and hydrological impact, *Int. J. Climatol.*, *26*, 2181–2198, doi:10.1002/joc.1359.

Hurowitz, J. A., W. W. Fischer, N. J. Tosca, and R. E. Milliken (2010), Origin of acidic surface waters and the evolution of atmospheric chemistry on early Mars, *Nat. Geosci.*, doi:2010/1038/ngeo831, in press.

Hynek, B. M. (2004), Implications for hydrologic processes on Mars from extensive bedrock outcrops throughout Terra Meridiani, *Nature*, *431*, 156–159, doi:10.1038/nature02902.

Hynek, B. M., and R. J. Phillips (2005), The etched terrain in Arabia Terra, Mars, is tilted, *Lunar Planet. Sci.*, *XXXVI*, Abstract 1222.

Hynek, B. M., and R. J. Phillips (2008), The stratigraphy of Meridiani Planum, Mars, and implications for the layered deposits' origin, *Earth Planet. Sci. Lett.*, *274*, 214–220, doi:10.1016/j.epsl.2008.07.025.

Hynek, B. M., R. E. Arvidson, and R. J. Phillips (2002), Geologic setting and origin of the Terra Meridiani hematite deposit on Mars, *J. Geophys. Res.*, *107*(E10), 5088, doi:10.1029/2002JE001891.

Knauth, P. L., D. M. Burt, and K. H. Wohletz (2005), Impact origin of the sediments at the Opportunity landing site on Mars, *Nature*, *438*, 1123–1128, doi:10.1038/nature04383.

Kring, D. A. (2007), *Guidebook to the geology of Barringer Meteorite Crater, Arizona*, LPI Contrib., 1355.

Laskar, J., A. C. M. Correia, M. Gastineau, F. Joutel, B. Levrard, and P. Robutel (2004), Long term evolution and chaotic diffusion of the insolation quantities of Mars, *Icarus*, *170*, 343–364, doi:10.1016/j.icarus.2004.04.005.

Lewis, K. W., O. Aharonson, J. P. Grotzinger, R. L. Kirk, A. S. McEwen, and T. -A. Suer (2008), Quasi-periodic bedding in the sedimentary rock record of Mars, *Science*, *322*, 1532–1535, doi:10.1126/science.1161870.

Lichtenberg, K. A., et al. (2010), Stratigraphy of hydrated sulfates in the sedimentary deposits of Aram chaos, Mars, *J. Geophys. Res.*, doi:10.1029/2009JE003353, in press.

Malin, M. C., and K. S. Edgett (2000), Sedimentary rocks of early Mars, *Science*, *290*, 1927–1936, doi:10.1126/science.290.5498.1927.

Manning, C. E., and S. E. Ingebritsen (1999), Permeability of the continental crust: Implications of geothermal data and metamorphic systems, *Rev. Geophys.*, *37*(1), 127–150, doi:10.1029/1998RG900002.

McCollom, T. M., and B. M. Hynek (2005), A volcanic environment for bedrock diagenesis at Meridiani Planum on Mars, *Nature*, *438*, 1129–1131, doi:10.1038/nature04390.

McLennan, S. M., et al. (2005), Provenance and diagenesis of the evaporite-bearing Burns formation, Meridiani Planum, Mars, *Earth Planet. Sci. Lett.*, *240*, 95–121, doi:10.1016/j.epsl.2005.09.041.

Moller, P., et al. (1997), Paleofluids and recent fluids in the upper continental crust: Results from the German Continental Deep Drilling Program (KTB), *J. Geophys. Res.*, *102*, 18,233–18,254, doi:10.1029/96JB02899.

Moore, J. M. (1990), Nature of the mantling deposit in the heavily cratered terrain of northeastern Arabia, Mars, *J. Geophys. Res.*, *95*, 14,279–14,289.

Moore, J. M., and D. E. Wilhelms (2001), Hellas as a possible site of ancient ice-covered lakes on Mars, *Icarus*, *154*, 258–276, doi:10.1006/icar.2001.6736.

Murchie, S. L., et al. (2009), Evidence for the origin of layered deposits in Candor Chasma, Mars, from mineral composition and hydrologic modeling, *J. Geophys. Res.*, *114*, E00D05, doi:10.1029/2009JE003343.

Neumann, G. A., M. T. Zuber, M. A. Wieczorek, P. J. McGovern, F. G. Lemoine, and D. E. Smith (2004), Crustal structure of Mars from gravity and topography, *J. Geophys. Res.*, *109*, E08002, doi:10.1029/2004JE002262.

Niles, P. B., and J. Michalski (2009), Meridiani Planum sediments on Mars formed through weathering in massive ice deposits, *Nat. Geosci.*, *2*, 215–220, doi:10.1038/ngeo438.

Noe Dobrea, E. Z., F. Poulet, and M. C. Malin (2008), Correlations between hematite and sulfates in the chaotic terrain east of Valles Marineris, *Icarus*, *193*, 516–534, doi:10.1016/j.icarus.2007.06.029.

Okubo, C. H., and A. S. McEwen (2007), Fracture-controlled paleo-fluid flow in Candor Chasma, *Mars, Science*, *315*, 983–985, doi:10.1126/science.1136855.

Okubo, C. H., et al. (2007), Deformation bands on Mars and implications for subsurface fluid flow, in *Seventh International Conference on Mars, July 9–13, 2007, Pasadena CA* [CD-ROM], *LPI Contrib., 1353*, abstract 3041.

Pelkey, S. M., et al. (2007), CRISM multispectral summary products: Parameterizing mineral diversity on Mars from reflectance, *J. Geophys. Res.*, *112*, E08S14, doi:10.1029/2006JE002831.

Phillips, R. J., et al. (2001), Ancient geodynamics and global-scale hydrology on Mars, *Science*, *291*, 2587–2591, doi:10.1126/science.1058701.

Poulet, F., R. E. Arvidson, C. Gomez, R. V. Morris, J.-P. Bibring, Y. Langevin, B. Gondet, and J. L. Griffes (2008), Mineralogy of Terra Meridiani and western Arabia Terra from OMEGA/MEx and implications for their formation, *Icarus*, *195*, 106–130, doi:10.1016/j.icarus.2007.11.031.

Putzig, N. E., M. T. Mellon, K. A. Kretke, and R. E. Arvidson (2005), Global thermal inertia and surface properties of Mars from the MGS mapping mission, *Icarus*, *173*, 325–341, doi:10.1016/j.icarus.2004.08.017.

Rossi, A. P., G. Neukum, M. Pondrelli, S. van Gesselt, T. Zegers, E. Hauber, A. Chicarro, and B. Foing (2008), Large-scale spring deposits on Mars?, *J. Geophys. Res.*, *113*, E08016, doi:10.1029/2007JE003062.

Saar, M. O., and M. Manga (2004), Depth dependence of permeability in the Oregon Cascades inferred from hydrogeologic, thermal, seismic, and magmatic modeling constraints, *J. Geophys. Res.*, *109*, B04204, doi:10.1029/2003JB002855.

Schultz, P. H., and A. B. Lutz (1988), Polar wandering on Mars, *Icarus*, *73*, 91–141, doi:10.1016/0019-1035(88)90087-5.

Sefton-Nash, E., and D. C. Catling (2008), Hematitic concretions at Meridiani Planum, Mars: Their growth timescale and possible relationship with iron sulfates, *Earth Planet. Sci. Lett.*, *269*, 366–376, doi:10.1016/j.epsl.2008.02.009.

Segura, T. L., O. B. Toon, A. Colaprete, and K. Zahnle (2002), Environmental effects of large impacts on Mars, *Science*, *298*, 1977–1980, doi:10.1126/science.1073586.

Smith, D. E., et al. (2001), Mars Orbiter Laser Altimeter (MOLA): Experiment summary after the first year of global mapping of Mars, *J. Geophys. Res.*, *106*, 23,689–23,722.

Squyres, S. W., and J. F. Kasting (1994), Early Mars: How warm and how wet?, *Science*, *265*, 744–749, doi:10.1126/science.265.5173.744.

Squyres, S. W., and A. H. Knoll (2005), Sedimentary rocks at Meridiani Planum: Origin, diagenesis, and implications for life on Mars, *Earth Planet. Sci. Lett.*, *240*, 1–10, doi:10.1016/j.epsl.2005.09.038.

Squyres, S. W., et al. (2006), Planetary science: Bedrock formation at Meridiani Planum, *Nature*, *443*, E1–E2.

Squyres, S. W., et al. (2009), Exploration of Victoria Crater by the Mars Rover Opportunity, *Science*, *324*, 1058–1061, doi:10.1126/science.1170355.

Stepinski, T. F., and A. P. Stepinski (2005), Morphology of drainage basins as an indicator of climate on early Mars, *J. Geophys. Res.*, *110*, E12S12, doi:10.1029/2005JE002448.

Tosca, N. J., S. M. McLennan, B. C. Clark, J. P. Grotzinger, J. A. Hurowitz, A. H. Knoll, C. Schroder, and S. W. Squyres (2005), Geochemical modeling of the evaporation processes on Mars: Insight from the sedimentary record at Meridiani Planum, *Earth Planet. Sci. Lett.*, *240*, 122–148, doi:10.1016/j.epsl.2005.09.042.

Tosca, N. J., A. H. Knoll, and S. M. McLennan (2008), Water activity and the challenge for life on early Mars, *Science*, *320*, 1204–1207, doi:10.1126/science.1155432.

Travis, B. J., N. D. Rosenberg, and J. N. Cuzzi (2003), On the role of widespread subsurface convection in bringing liquid water close to Mars' surface, *J. Geophys. Res.*, *108*(E4), 8040, doi:10.1029/2002JE001877.

Wang, C. -Y., M. Manga, and J. C. Hanna (2006), Can freezing cause floods on Mars, *Geophys. Res. Lett.*, *33*, L20202, doi:10.1029/2006GL027471.

Weitz, C. M., M. D. Lane, M. Staid, and E. Z. Noe Dobrea (2008), Gray hematite distribution and formation in Ophir and Candor chasmata, *J. Geophys. Res.*, *113*, E02016, doi:10.1029/2007JE002930.

Williams, R. M. E. (2007), Global spatial distribution of raised curvilinear features on Mars, *Lunar Planet. Sci.*, *XXXVIII*, Abstract 1338.

Wiseman, S. M., et al. (2008), Phyllosilicate and sulfate-hematite deposits within Miyamoto crater in southern Sinus Meridiani, *Geophys. Res. Lett.*, *35*, L19204, doi:10.1029/2008GL035363.

Wiseman, S. M., R. E. Arvidson, R. V. Morris, F. Poulet, S. L. Murchie, F. P. Seelos, J. L. Bishop, J. C. Andrews-Hanna, D. Des Marais, and J. L. Griffes (2010), Spectral and stratigraphic mapping of hydrated sulfate and phyllosilicate-bearing deposits in northern Sinus Meridiani, Mars, *J. Geophys. Res.*, doi:10.1029/2009JE003354, in press.

J. C. Andrews-Hanna, Department of Geophysics, Colorado School of Mines, 1500 Illinois St., Golden, CO 80401, USA. (jcahanna@mines.edu)

R. E. Arvidson and S. M. Wiseman, Department of Earth and Planetary Sciences, Washington University in St. Louis, Campus Box 1169, 1 Brookings Dr., St. Louis, MO 63130, USA.

M. T. Zuber, Department of Earth, Atmospheric, and Planetary Sciences, Massachusetts Institute of Technology, Cambridge, MA 02139, USA.